DIETARY ACCUMULATION OF HEXABROMOCYCLODODECANE DIASTEREOISOMERS IN JUVENILE RAINBOW TROUT (*Oncorhynchus mykiss*); Bioaccumulation/Depuration Parameters and Evidence of Bioisomerization

By
Kerri Lynn Law

A Thesis submitted to the Faculty of Graduate Studies in Partial Fulfillment of the Requirements for the Degree of MASTER OF SCIENCE

Chemistry Department
University of Manitoba
Winnipeg, Manitoba
2006

ABSTRACT

The major objectives of this research were to examine the bioaccumulation parameters [depuration rates (k_d), half life ($t_{1/2}$) and biomagnification factor (BMF)] of individual isomers of hexabromocyclododecane (HBCD, $C_{12}H_{18}Br_6$) in fish and to test the hypothesis of *in vivo* bioisomerization. This was done by exposing three groups of juvenile rainbow trout (*Oncorhynchus Mykiss)* to food fortified with known concentrations of an individual diastereoisomer (α–, β–, γ–) for 56 days (uptake phase) followed by 112 days (depuration phase) of unfortified food. A fourth group of fish were exposed to unfortified food for the duration of the experiment. Fish (*n=4*) from all four aquaria were sacrificed on days 0, 7, 14, 56, 63, 70, 112 and 168 and muscle tissue was extracted and analyzed for diastereoisomer concentrations by high performance liquid chromatography tandem mass spectrometry (LC/MS/MS).

Bioaccumulation of the γ–diastereoisomer was linear during the uptake phase while the α– and β–diastereoisomers were found to increase exponentially with respective doubling times of 14.1 and 20.5 days. Both the β– and γ–diastereoisomers followed first order depuration kinetics with calculated $t_{1/2}$'s of 94 ± 25 and 84 ± 51 (± 1 × standard error) days, respectively. The BMF for the α–diastereoisomer (BMF = 4.1) was one and a half times greater than the β-diastereoisomer (BMF = 2.6) and about one fifth larger than the γ-diastereoisomer (BMF = 3.6). The large BMF for the α–diastereoisomer is consistent with this diastereoisomer dominating higher trophic level organisms in wildlife. Although the BMF of the β–diastereoisomer suggests that it will biomagnify, because it is present in small quantities in commercial mixtures it is rarely detected in

environmental samples. Results from these studies also provide evidence of bioisomerization of the β– and γ–diastereoisomers. Most importantly, the α–diastereoisomer which was recalcitrant to bioisomerization by juvenile rainbow trout in this study and known to be the dominant diastereosiomer in fish, was bioformed from both the β– and γ–diastereoisomers. To our knowledge, this is the first report of bioisomerization of a halogenated organic pollutant in biota.

ACKNOWLEDGEMENTS

I would like to thank my supervisor, Gregg Tomy, for taking me on as a graduate student. Thank you for constantly taking time out of your work to give me your full undivided attention when I needed guidance and reassurance in what I was doing. You have been an excellent source of knowledge and you have made my Masters experience a great one- no working past 4:30 pm (at the latest), no work to take home, time off when I needed/wanted it…how could I complain! Thanks for never allowing me to get bored and making sure there was always something for me to do…even if it meant passing off one of your jobs onto me! Thanks for everything!

If it wasn't for Thor Halldorson I would still be in the laboratory trying to figure out what to do with my fish samples! Thanks Thor for teaching me everything I needed to know about extracting, analyzing and quantifying brominated flame retardants in fish, giving me the fancy spreadsheets that made my life somewhat easier in quantifying all my data (if I only entered the proper equation from the start!) and for taking me step-by-step through the LC/MS/MS so I would be able to run it myself. I also have to thank you for allowing me to interpret gibberish (i.e., your hand writing) I truly believe that I now have the experience to decipher any code that comes by my desk!

Bob Danell, what can I say, thank you for teaching me how to work with difficult people and making it enjoyable! You gave me a lot of pointers in good laboratory practice, and you always kept me on the ball.

Thank you to the fish sacrificing crew; Bob Evans, Kerry Wautier, Bob Danell, Thor Halldorson, Vince Palace, Lindon Brinkworth -- if it weren't for you guys, I would still be sacrificing fish!

To everyone else at FWI who I worked with; thanks for the friendships and making the past 2 years enjoyable and memorable ones.

To my committee, Vince Palace and John Westmore, thank you for the valuable comments on my thesis. Thank you to Environment Canada's Existing Substances Branch for the partial funding for my thesis.

To my two sister; Tara and Cristy, thanks for always setting higher standards for me by Tara finishing your Masters (please don't do a PhD…I have had enough school) and Cristy for never having a grade lower than an A! Also, I have to thank them for the great car pool…you guys made the ride to and from school a joy, especially on snack Fridays!

To my mom and dad, thanks for encouraging me to reach for my goals and always being proud of me for what I accomplish. My parents always said that us three girls could live at home for free as long as we were going to school, so I have to thank them for the room and board and mom's cleaning and laundry service for the past 25 years! I know my mom can't wait for me to leave as she already has me packed up!

To my husband, David Pleskach, thanks for sticking by me through all of my years of school and for encouraging me to "stop goofing around and hurry up and finish" and yes, I will now look for a 'real job'!

Lastly, to the fish who sacrificed their lives for the love of science to make this project work (even though they had no choice).

To family, for all of their support and encouragement

throughout my university career,

TABLE OF CONTENTS

LIST OF TABLES

LIST OF FIGURES

ABBREVIATIONS AND SYMBOLS

$^{13}C_{12}$– labelled carbon 13

a.u.– arbitrary unit

α– alpha HBCD isomer [RR,SR,RS]

β– beta HBCD isomer [RR,SR,SR]

BFR– brominated flame retardant

BMF– biomagnification factor

CA- corrected area

d_{18}– deuterium

d.c.– direct current

DCM– dichloromethane

d_t– doubling time

γ– gamma HBCD isomer [RR,RS,SR]

g– grams

HBCD– hexabromocyclododecane

HPLC– High performance liquid chromatography

k´– partition coefficient

k_d– depuration rate constant

LC– liquid chromatography

LIPMIS– labelled instrument performance matrix internal standard

LRIS– labelled recovery internal standard

m/z– mass to charge ratio

MS– mass spectrometer

MS/MS– tandem mass spectrometer

ng– nanograms

PBDE– polybrominated diphenyl ether

pg– picograms

QA/QC– Quality assurance./Quality control

rec– recovery

r.f– radio frequency (alternating current)

SA– sample

STD– standard

t_o– dead time

t_r– retention time

$t_{1/2}$– half-life

Σ– total

CHAPTER 1

INTRODUCTION

1.1. LITERATURE REVIEW OF HEXABROMOCYCLODODECANE.

There are three main groups of flame retardants; organic halogens, phosphorus compounds, and metal compounds. There are more than 175 classified flame retardants, 75 of them being brominated. The most commonly used flame retardants are the brominated flame retardants (BFRs) due to their high efficiency, low decomposing temperature and low cost (*1,2*).

Hexabromocyclododecane (HBCD, $C_{12}H_{18}Br_6$) is the most widely used aliphatic BFR and the third in global production volume following tetrabromobisphenol A and polybrominated diphenyl ethers (PBDEs). In 1999 the global demand for HBCD (~16 kilotons) was almost double that of the pentabromodiphenyl ether mixture (~8.5 kilotons) (*3,4*). In Europe, HBCD has begun to replace some PBDEs in their applications (*1*).

There are two types of flame retardants; reactive and additive. Reactive flame retardants are covalently bonded to the polymer and additive flame retardants are added as a component of the dissolved material. HBCD is an additive flame retardant, like the PBDEs. Being an additive flame retardant, there is the risk that HBCD can leach into the environment after disposal of the product; other sources of release include during production and manufacturing of the final product.

1.1.1. INDUSTRIAL SYNTHESIS OF HBCD

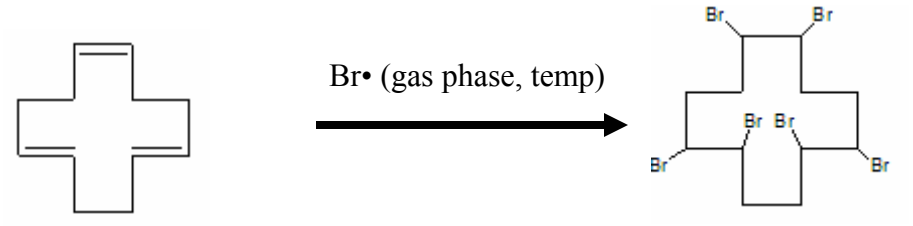

Figure 1.1. Synthesis of technical HBCD by bromination of 1, 5, 9–cyclododecatriene.

1,2,5,6,9,10-hexabromocyclododecane is synthesized by high temperature gas phase bromination of 1Z, 5E, 9E-cyclododecatriene (Figure 1.1) (*5*). The resulting technical mixture consists primarily of three isomers; α–, β– and γ–HBCD (Figure 1.2). [The assignment of Greek letters is based on their elution order from a reverse phase high performance liquid chromatography column.]

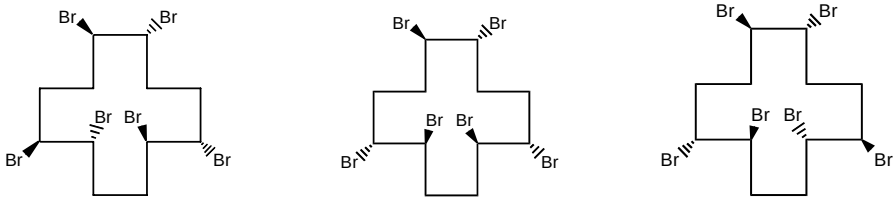

Figure 1.2. Structures of the α–, RR,SR,RS (left), β–, RR,SR,SR (middle) and γ–, RR,RS,SR (right) HBCD isomers (*6*).

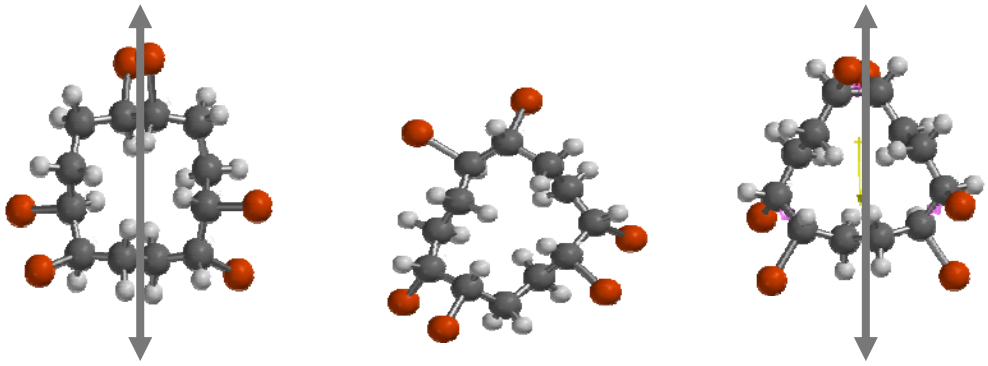

Figure 1.3. Three-dimensional structures of α– (left), β– (center), and γ– (right) HBCD isomers (*7*).

The 3-dimensional views of the isomers (Figure 1.3) show that the α– and γ–isomers both have a C_2 axis of symmetry while β–HBCD does not. This suggests that there could be difference in the chemical properties amongst the isomers.

The proportions of the isomers in the technical mixture are dependent on the final synthetic process. Industrially, there are four different technical mixtures of HBCDs: low melt, medium range, high melt and thermal stabilized (*5*). Overall, the average approximate proportions of each isomer in each technical mixture is 6, 8, and 80% for α– , β– and γ–HBCD, respectively (*8*). What makes each technical mixture different is the percent of γ-HBCD present, which ranges from ~70-90%. The selection of HBCD grade used depends on the usage of the end-product.

1.1.2. PHYSICAL AND CHEMICAL PROPERTIES

Technical HBCD is a solid, white powder at room temperature (*9*). Physicochemical properties of HBCD are as follows: molecular weight of 641.7 g/mol; melting point ranges from 185-195^{o}C and depends on the isomer ratio and impurity composition; vapour pressure of 4.7 x 10^{-7} mm Hg (at 25^{o}C) and the log octanol water partition coefficient (log K_{ow}) of 5.6 (*9*). Until recently, all physicochemical property measurements were done on the technical mixture as individual isomers have not been readily available.

The water solubility of α–HBCD has been recently measured and found to be one order of magnitude greater than β–, and γ–HBCD (Table 1.1). The fact that HBCD has similar physiochemical properties to other persistent organic pollutants such as polychlorinated biphenyls (PCBs) and PBDEs, suggests that HBCD may be persistent, bioaccumulative and toxic (*10*).

Table 1.1. Water solubility of HBCD isomers (*11,12*).

	Technical mixture	α- HBCD	β-HBCD	γ-HBCD
Water solubility (μg/L)	3.4	48.8	14.7	2.08

1.1.3. USES AND APPLICATIONS

HBCD is the principal flame retardant in extruded (XEPS) and expanded (EPS) polystyrene foams used as thermal insulation in the building industry. The amount of HBCD in plastics ranges from 0.5 to 7%, depending on the type of plastic (*10*). Extruded polystyrene contains ~1-2% HBCD (*13*). Secondary uses of HBCD include residential and commercial upholstery textiles and electronics.

Our group extracted HBCD from DOW expanded polystyrene foam insulation, purchased from a local hardware store, by using a method similar to Zitko (*14*) and found that all three isomers were present in the insulation (Figure 1.4) in relative amounts of α–: 59.2%; β–: 23.3%; γ–: 17.5%. It is noteworthy that the γ–isomer is no longer the dominant isomer in this final product. This is consistent with the literature which suggests that the isomeric composition of the technical HBCD mixture changes during application of the flame retardant (*5,15*). For example, when the technical mixture is incorporated into XEPS or EPS, temperatures above 160^{o}C are employed and this effectively changes the abundances of the α– and γ–isomers. The thermal rearrangement or isomerization of HBCD isomers has been examined (*5*). Interestingly, they found that between 160–200^{o}C the α–isomer becomes the most predominant isomer (~78%). This result was also independent of the isomer ratio of the starting material. So whereas the γ–isomer is dominant in the technical mixture at room temperature, during elevated temperatures (such as those present during XEPS and XPS processing), a rearrangement occurs resulting in a predominance of the α–isomer (*5*).

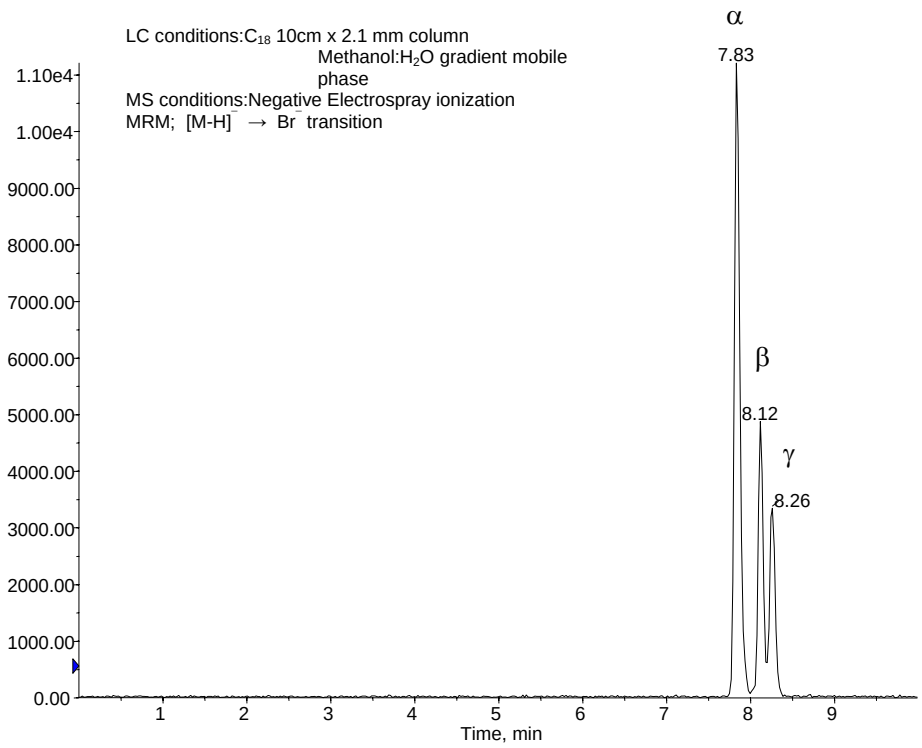

Figure 1.4. HPLC chromatogram of solvent extract of DOW expanded polystyrene foam insulation showing the presence of all three HBCD isomers.

An estimation for the global demand for HBCD in 2001 is shown in Table 1.2.

Table 1.2. An estimate of the world market for HBCD in 2001 (*16*)

Country	**Usage (metric tons)**
United States	2800
Europe	9500
Asia	2200
Worldwide use	16700

1.1.4. INHIBITION PROCESS OF A BROMINATED FLAME RETARDANT

A flame retardant is added to a variety of products to slow down the burning process or to delay the ignition or combustion of the product. In order for a flame retardant to work, it must interfere with one of the three elements required for combustion; heat, fuel or oxygen (Figure 1.5).

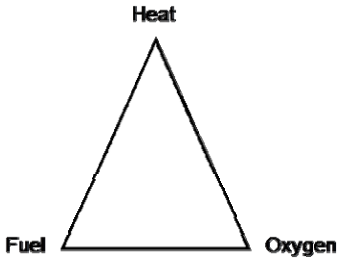

Figure 1.5. Fire triangle (*17*).

There are four stages during a fire; ignition, propagation, steady combustion and termination, and a flame retardant can interfere at any of these stages (Figure 1.6) (*17*).

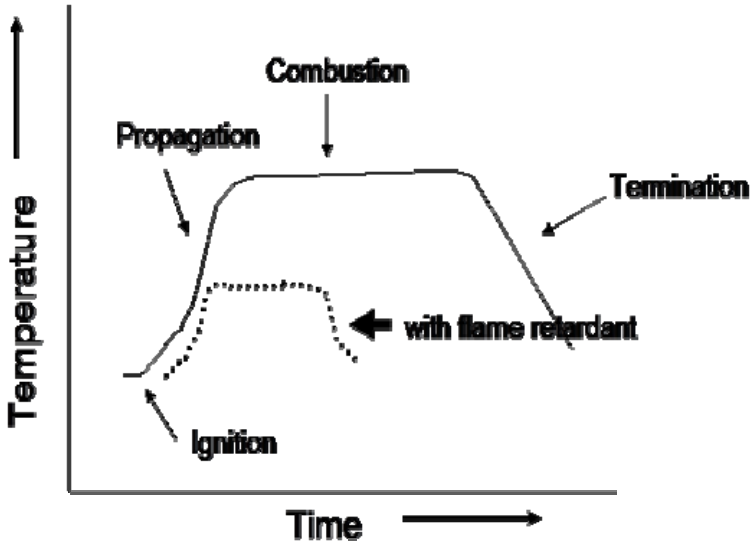

Figure 1.6. Stages of the life cycle of a fire and the effect of a flame retardant on a fire (*17*).

When BFRs absorb the required amount of energy (heat), the carbon-bromine bond breaks, forming bromine radicals. The bromine radical reacts with the hydrogen atoms in the polymer or captures free hydrogen atoms to form HBr (*17*).

$$RH + Br\bullet \rightarrow HBr + R\bullet, \text{ where RH is the polymer.} \quad [1\text{-}1]$$

$$\bullet H + Br\bullet \rightarrow HBr \quad [1\text{-}2]$$

HBr slows down the chain reactions that take place during the burning process. One example of this is the deactivation of hydroxyl radicals; (*17*)

$$\cdot OH + HBr \rightarrow H_2O + \cdot Br \quad [1\text{-}3]$$

The overall effect is that the bromine atom withdraws energy from the combustion-propagation stage of the fire, slowing the burning process (*17*).

A good flame retardant should be inexpensive, stable to heat, colorless, easily blended in with the polymer, should decompose around the same temperature as the polymer, must not change physical and mechanical properties once it is in the final product, must be stable at temperatures that the product is formed at, and does not release toxic substances into the environment (*17*).

1.1.5. ENVIRONMENTAL LEVELS AND TOXICOLOGY

HBCD is a ubiquitous global contaminant that has been detected in the atmosphere, sewage sludge, soils and sediments, human breast milk and serum, and biota; birds, fish (farmed and wild), benthic invertebrates, marine mammals and zooplankton (in Bergman (*18*) and Law *et al. (19)* [and references therein]).

As stated earlier, possible emission sources of HBCD into the environment include; manufacturing, use and disposal (*10*). Emissions during manufacturing can be by air, but due to HBCDs low volatility, emissions are more likely to occur with the release of plastic dust (*10*). Because it is an additive flame retardant, HBCD can leach from the material it has been impregnated into during the lifetime of the product. This can occur over a long period of time, as some products have long lifetimes. After disposal of a

product in a landfill or during recycling it is possible for HBCD to leach into the air (particle bound) and water (surface and ground) (*10,20*).

HBCD has been quantified in sewage treatment plant sludge, which suggests that HBCD is associated with suspended particulate material and can be removed during the wastewater treatment process (*20*).

Sellstrom *et al*. showed that HBCD is bioavailable by quantifying HBCD in pike captured near textile factories along the River Viskan in Sweden (*21*). A recent study done by Tomy *et al*. on the Lake Ontario food web, found that the α–isomer was dominant in pelagic fish; the γ–isomer was consistently lower than the α–isomer while the β–isomer was below detection limits in the samples (*6*). Even though the β–isomer is present in the technical mixture, it is detected at the smallest concentrations in the environment.

Zegers *et al*. recently showed that the α–isomer dominated profile in higher trophic level organisms is due in part to a stereoisomer-specific biotransformation mediated by cytochrome P450 enzymes (*22*). Using an *in vitro* system that employed microsomes from a harbour seal, the authors showed that the β– and γ–HBCD isomers were rapidly biotransformed to their respective hydroxylated metabolites while the α–isomer remained unaffected (*22*).

Our group also studied the extent of bioaccumulation of HBCD in Lake Winnipeg's food web by analyzing six species of fish, zooplankton, mussels, sediment and water from the south basin of the lake (*23*). We found a significant positive correlation between the concentration of total (Σ) HBCD ($p<0.0001$) and the lipid content in fish (*23*). The concentration of ΣHBCD ranged from 1.22 – 15.71 ng/g (lipid weight (lw)) for α-HBCD, 0.53 – 5.58 ng/g (lw) for β-HBCD, and 1.03 – 44.13 ng/g (lw) for γ-HBCD (*23*). Concentration of α–HBCD in water was 11 ± 2 pg/L and γ–HBCD was 2.89 $\pm$ 0.9 pg/L, while β-HBCD was below its method detection limit (MDL) (*23*). The γ–HBCD, which is the most hydrophobic of the three diastereoisomers, was detected at concentrations of 50 ± 20 pg/g (dw) in sediment, while α– and β–HBCD isomers were below their respective detection limits (*23*).

HBCD exposure has been linked to sub-lethal and biochemical effects, including increased activity of the antioxidant enzyme catalase and an increase in relative liver size (*24*). Both of these effects are consistent with peroxisome proliferators (*24*). HBCD can also inhibit CYPIA enzymes, a group of important detoxification enzymes (*24*). The technical HBCD mixture has been linked to carcinogenesis by inducing intragenic recombination in mammalian cells, similar to PCBs (*25*).

HBCD has been reported to be absorbed from the gastrointestinal tract and then accumulates in the adipose tissue, therefore it is suggested that food intake is the largest single source of human exposure (*26*). HBCD intake is mostly from fish, and the estimated intake is approximately three times greater than PBDEs (*27*).

1.2. ANALYTICAL METHODS FOR HBCD

Information on the environmental fate and behaviour of the individual diastereoisomers is beginning to emerge. This is partly attributable to recent measurements of HBCD based on HPLC/MS. Using HPLC electrospray tandem mass spectrometry (ESI-MS/MS), it is now possible to separate the individual isomers using a method first developed by Budakowski and Tomy (*28,29*) and later refined by Tomy *et al*. (*29*).

Early analysis of HBCD relied on gas chromatography (GC), which precluded determination of specific diastereoisomer concentrations. HBCD isomers are thermally labile and analysis of the individual isomers by GC and detection by mass spectrometry in the electron capture negative ion mode (GC/ECNI-MS) resulted in one broad peak (*30*), or in significant amounts of degradation (Figure 1. 7). Figures 1.8 – 1.10 show results for the three HBCD isomers when analyzed individually by HPLC/ESI-MS/MS and GC/ECNI-MS. HPLC/ESI-MS/MS results in single well-resolved peaks in each case. When individual isomers were analyzed by GC/ECNI-MS significant amounts of degradation products were observed.

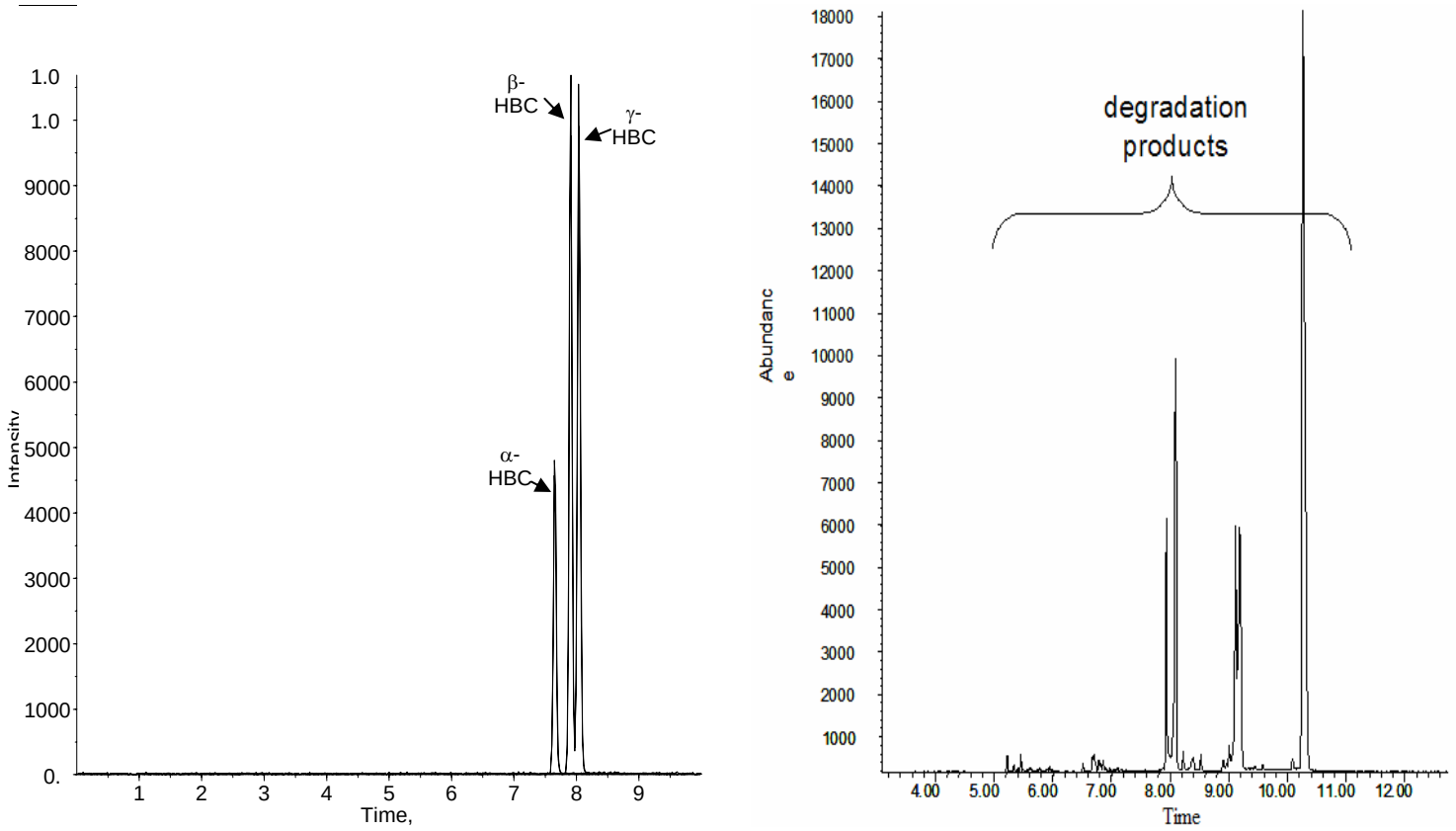

Figure 1.7. 100 pg/μL native HBCD isomer standard mix analyzed by HPLC-MS-MS (left) and by GC-MS (right)

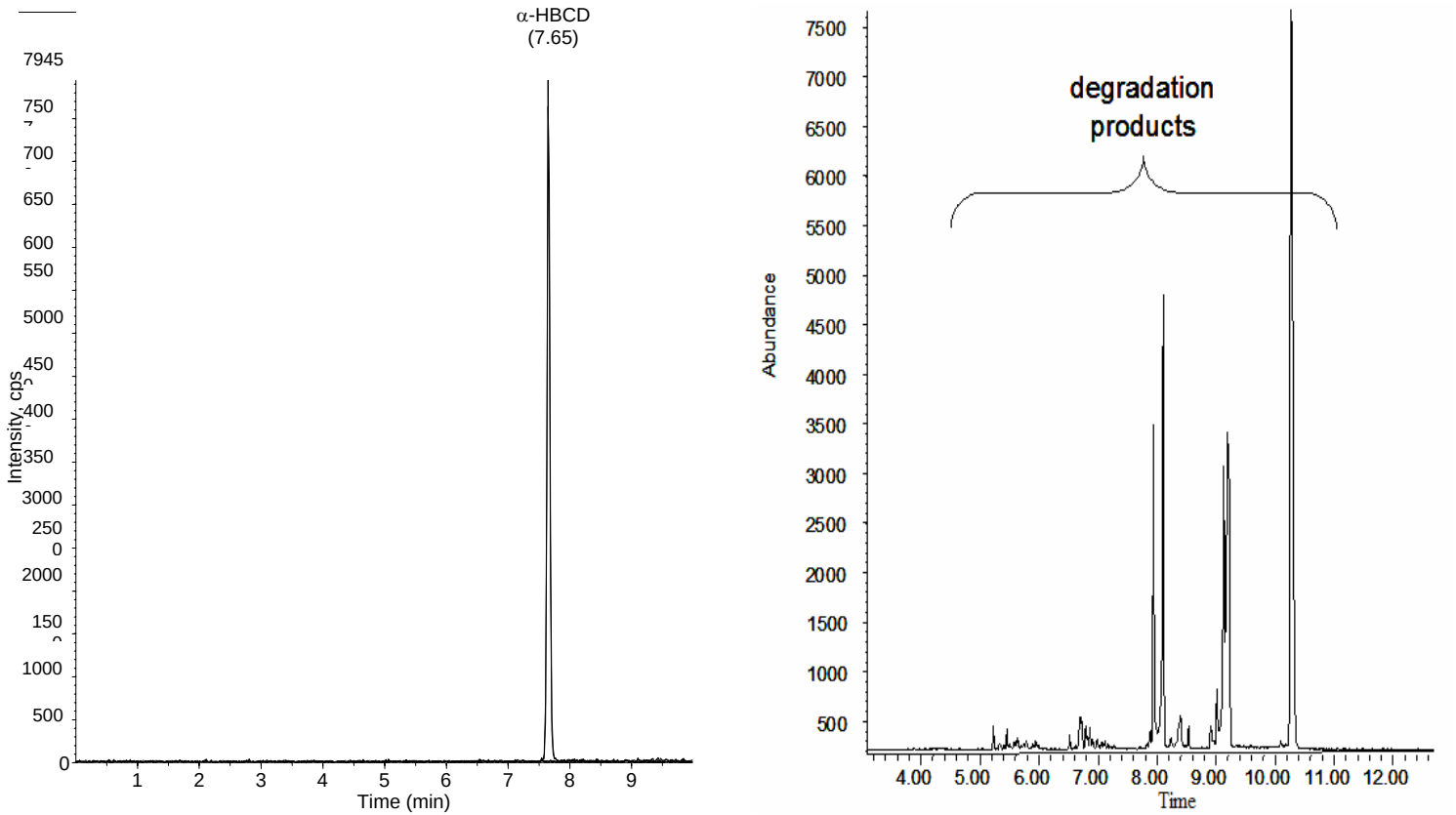

Figure 1.8. 100 pg/μL native α-HBCD standard analyzed by HPLC-MS-MS (left) and by GC-MS (right)

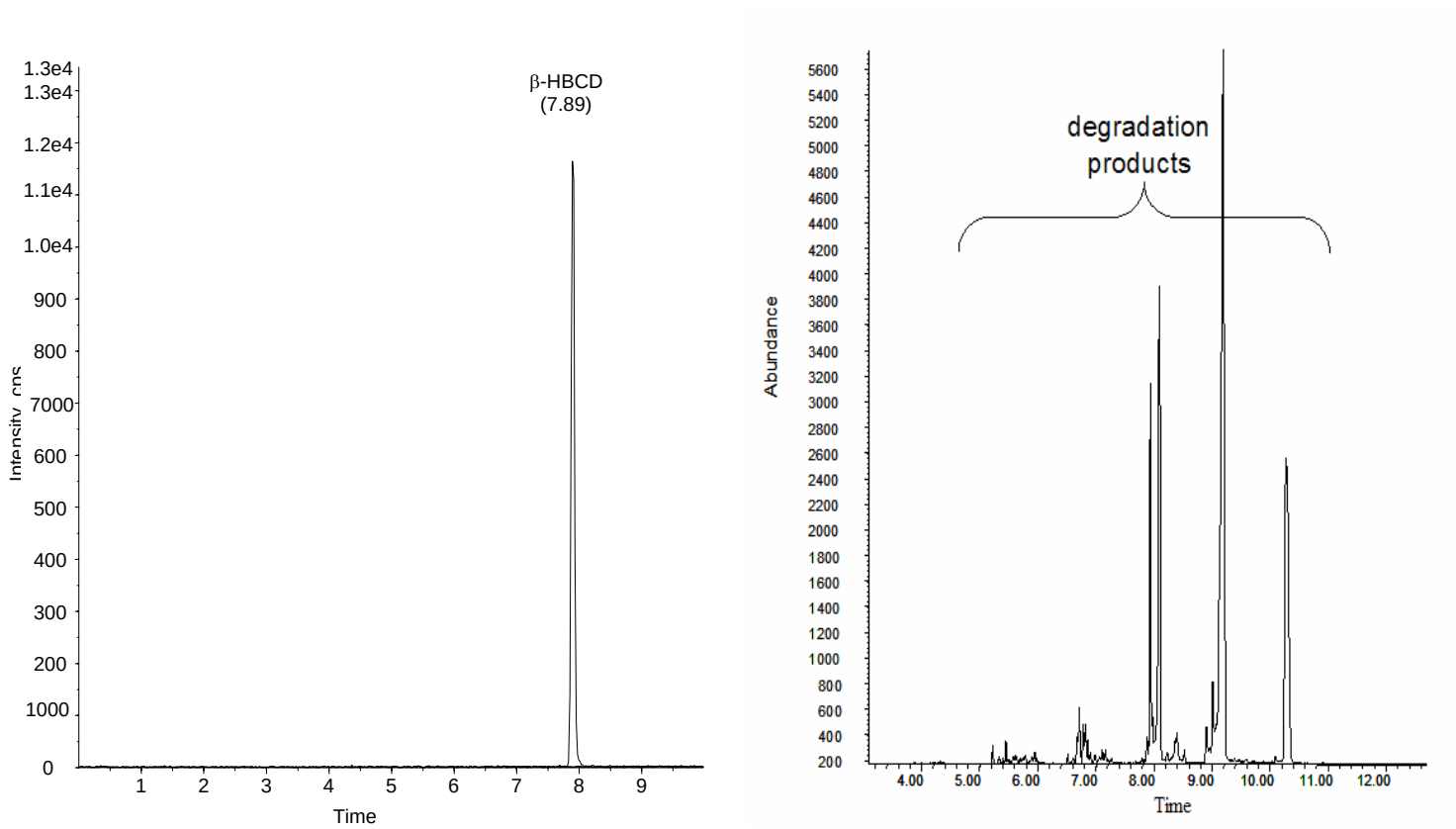

Figure 1.9. 100 pg/μL native β-HBCD standard analyzed by HPLC-MS-MS (left) and by GC-MS (right)

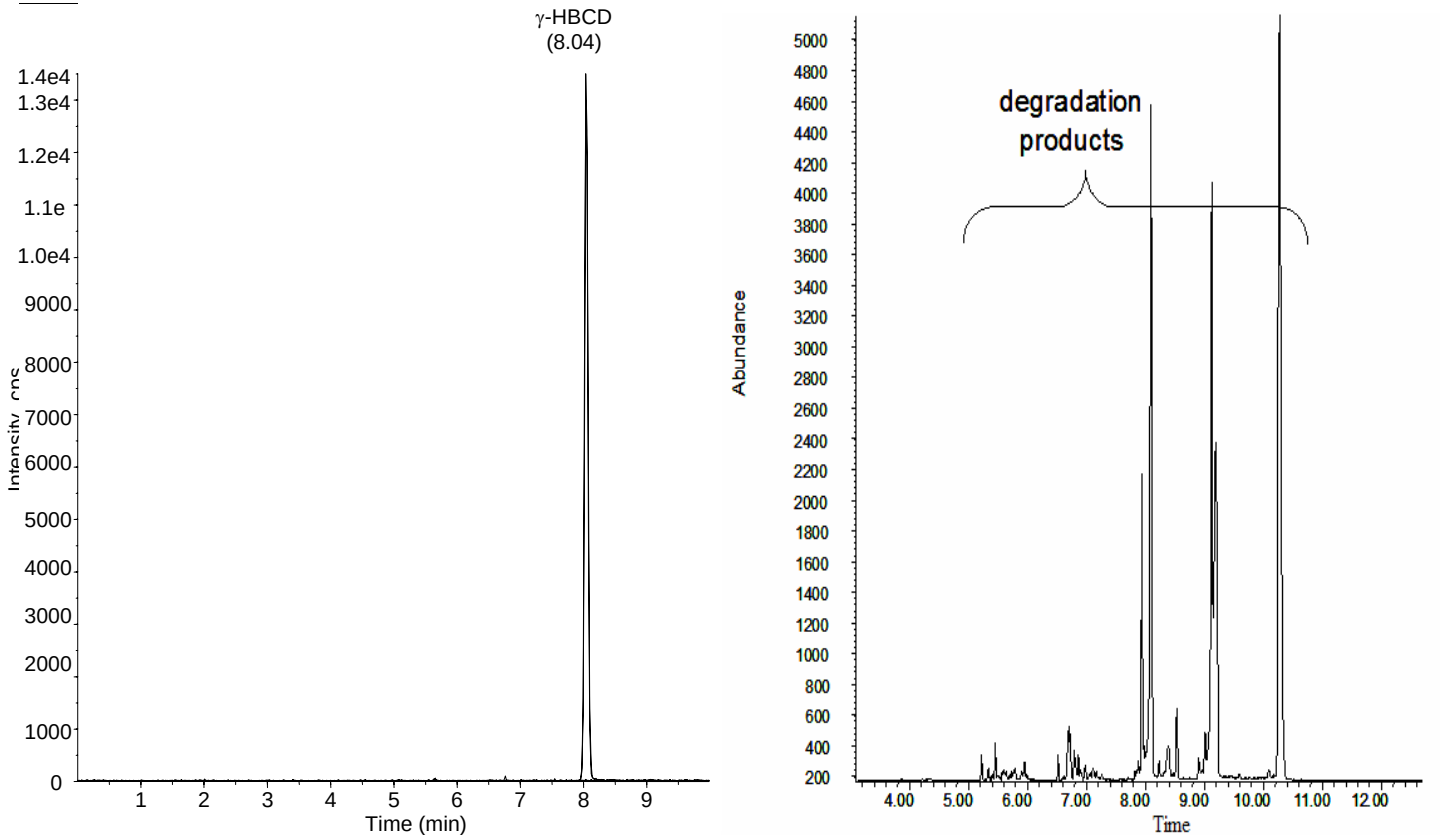

Figure 1.10. 100 pg/μL native γ-HBCD standard analyzed by HPLC-MS-MS (left) and by GC-MS (right)

1.3. OBJECTIVES OF PRESENT RESEARCH

The primary objectives of this study were to test the hypothesis of bioisomerization in fish and also to examine bioaccumulation parameters of the individual diastereoisomers. The experimental design was similar to our previous study examining kinetics of PBDEs (*31*) and is described in detail in the Experimental Section.

Chapter 2

ANALYTICAL INSTRUMENTATION

2.1. HIGH PERFORMANCE LIQUID CHROMATOGRAPHY

High performance liquid chromatography (HPLC) can be used to separate non-volatile components in a sample. HPLC consists of mobile phase reservoirs, a set of pumps, an injector, a column and a detector. The solvents used should be pure, readily available, acceptable level of toxicity, low viscosity and must dissolve the sample components completely without reacting with them (*32*). The pumps provide a constant flow rate. The pump used in this experiment was a reciprocating pump. The components in a liquid sample extract are separated by establishing conditions on the HPLC column so that the individual components of the extract will elute off the column at different rates. The rate of elution is influenced by the polarity of the mobile phase (liquid phase) and the stationary phase (solid phase). There is reverse phase and normal phase chromatography, in this experiment, reverse phase was used so it will be described in detail.

2.1.1. REVERSE PHASE

In reverse phase chromatography, the stationary phase is non polar and the mobile phase is polar (Figure 2.1). We used a silica stationary phase with a C_{18} aliphatic chain (octadecyl, $-(CH_2)_{17}-CH_3$). In the sample, any non-polar analytes will be retained on the column and any polar or ionic analytes are eluted from the column rapidly, along with the mobile phase (*33-35*). The non-polar analytes will remain fixed to the stationary phase

until the mobile phase becomes more non-polar. The analyte partitions itself between the polar mobile phase and the non-polar stationary phase (column packing) based on their respective polarities (*33,34*).

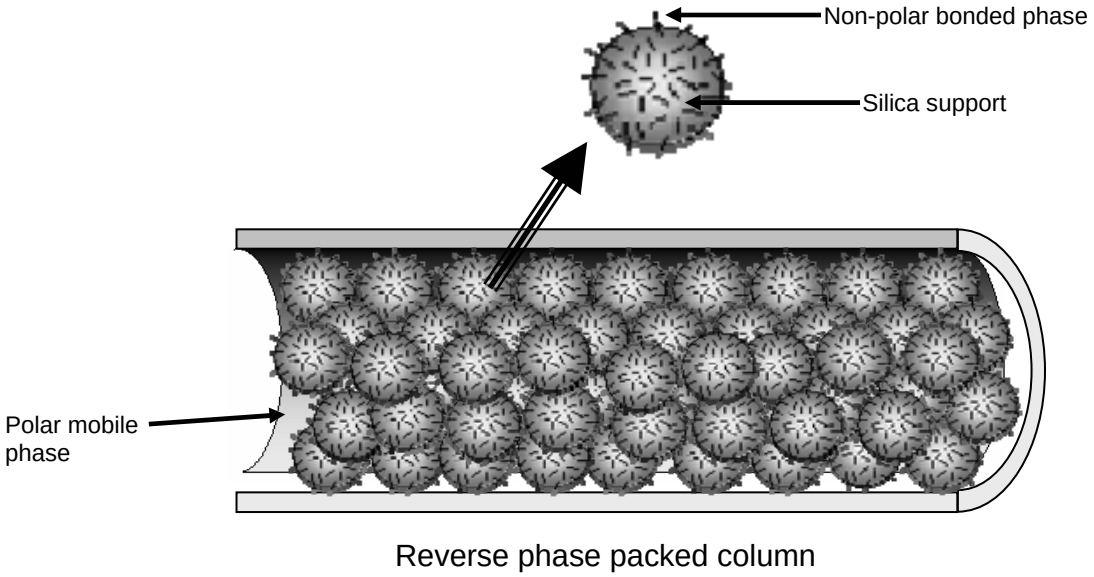

Figure 2.1. Schematic of reverse phase liquid chromatography column (*33*).

2.1.2. RETENTION TIME

The retention time is the time it takes the analyte to elute from the column and it depends on the solubility, adsorption, size and ionization characteristics of the analyte and the specific parameters of the HPLC (*34*). The retention time also varies with the length of the column and the flow rate of the mobile phase (*35*). The analyte can bond to the stationary phase by: hydrogen bonding, van der Waals' forces, electrostatic forces or hydrophobic forces (*32*).

Retention time (t_r) is the sum of the time that there is no interaction between the samples and the column packing, called dead time (t_o), plus the time needed for the sample to elute from the column (Figure 2.2). Because retention time varies with many factors, one uses the relative partition coefficient (k') which relates t_r and t_o at a constant flow rate.

$$k' = \frac{(t_r - t_0)}{t_0} \quad [2\text{-}1]$$

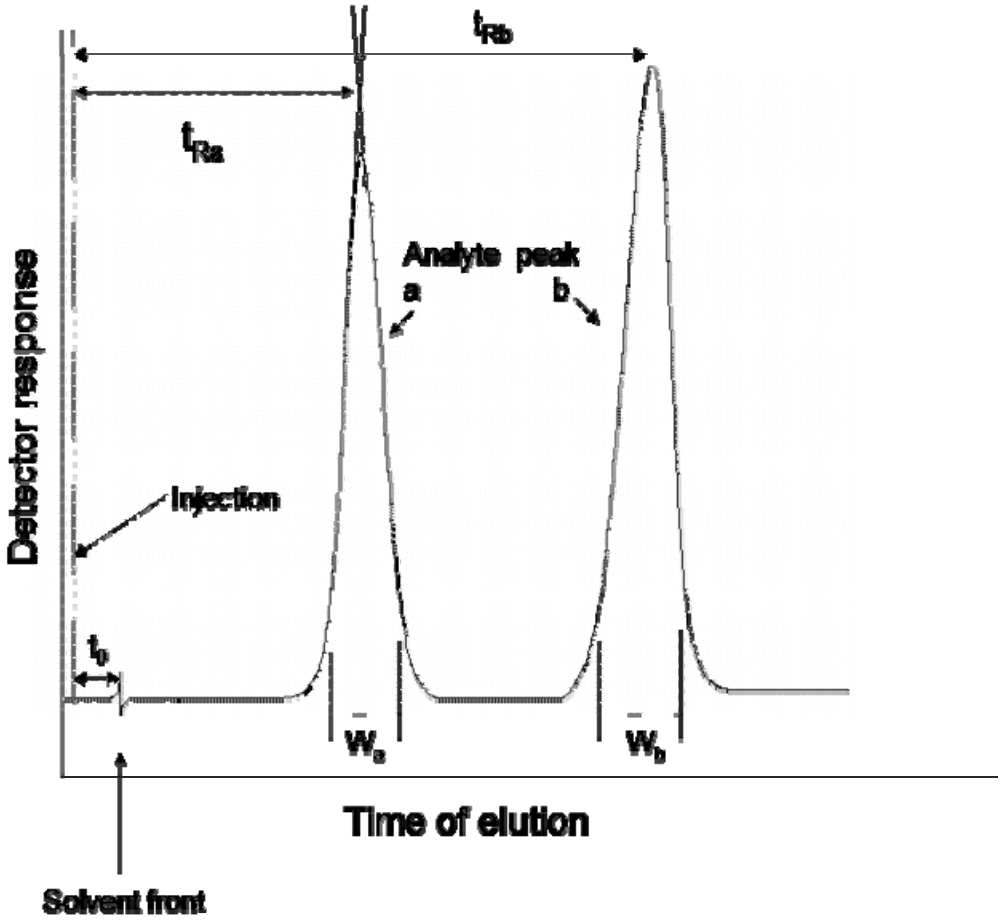

Figure 2.2. Measurement of retention time and resolution of analyte peaks a and b (*34*).

2.1.3. RESOLUTION

Resolution is the degree to which separation of the components on the column takes place. Complete resolution of two components occurs when the peaks do not overlap. It will increase with the use of a smaller diameter of packing material in the column. Resolution can be calculated by:

$$\text{Resolution}=\frac{(t_{rb}-t_{ra})}{0.5(W_b+W_a)} \quad [2\text{-}2]$$

Where, t_{rb} and t_{ra} are the retention times of peaks b and a, respectively. W_a and W_b are the width of peaks a and b, respectively, at the base.

2.2. INTERFACING

The analyte elutes from the analytical column as a liquid, but must be in ion form before entering the MS. Therefore, there has to be an interface between the HPLC and MS that removes the mobile phase and ionizes the analyte. There are many types of interfaces that are used today: thermospray ionization (TSP), electrospray ionization (ESI) and atmospheric pressure chemical ionization (APCI). The one that was used in our studies was ESI, therefore it will be the only one discussed in this thesis.

2.2.1. ELECTROSPRAY IONIZATION

Electrospray ionization produces gas phase ions at atmospheric pressure. The sample enters the ESI source through an electrospray needle which has a high electrical potential relative to a metal plate (counter electrode) in front of the needle exit, producing an aerosol spray of highly charged droplets (*33,35,36*). The needle potential can either be positive or negative, producing either positive or negative ions, respectively. For example, if the solution contains preformed ions and the needle is negative with respect to the counter electrode then cationic species within the solution are attracted to the inner surface of the electrospray needle (*36*). Under the influence of the electric field the emerging solution breaks up into droplets with the negative species tending to migrate towards the side of the ion droplet closest to the orifice plate (*36*). The negative charges

at the surface of the ion will repel each other, thus increasing the surface area of the ion and elongating the ion away from the needle (*36*).

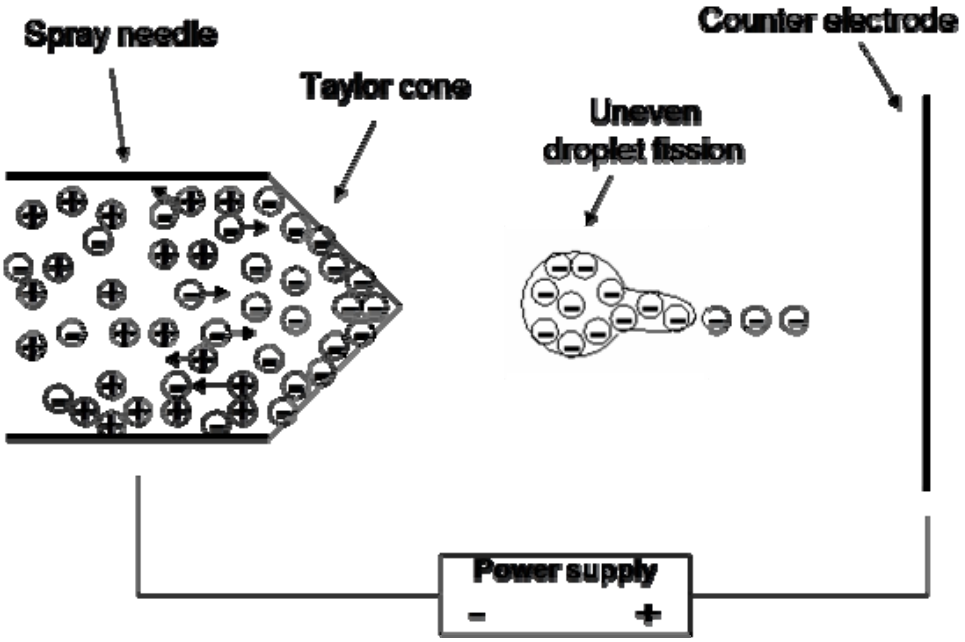

Figure 2.3. Charge separation and droplet fission in an ESI source (*36*).

A continuous (counter current, heated) stream of nitrogen flows through the source which initiates desolvation (the evaporation of the solvent) (*35,36*).

As the size of the droplet decreases, the charge density of the droplet increases and the repulsive forces of the charges on the surface will overcome the cohesive forces of the surface tension (*35*). A 'Coulombic explosion' occurs forming many smaller charged droplets from the parent droplet (*35*). If the electrospray needle has a positive potential, the same process occurs, but with opposite charge.

Many neutral solutes can undergo proton transfer reactions in the needle. Single $[M\pm H]^{\pm}$, and multiple $[M\pm nH]^{n\pm}$ ions can be formed in this way. The amount of charge (n) usually increases with the molecular mass. In this study $[M-H]^{-}$ ions were used.

The ions are then pulled into the high vacuum region of the source, through an orifice and then travel through a set of skimmer plates which are at different pumping stages and have different ion optics; both help to maximize the ion transmission to the mass spectrometer (*36*). Their kinetic energy is reduced to~50 eV before they enter the mass spectrometer (Figure 2.4).

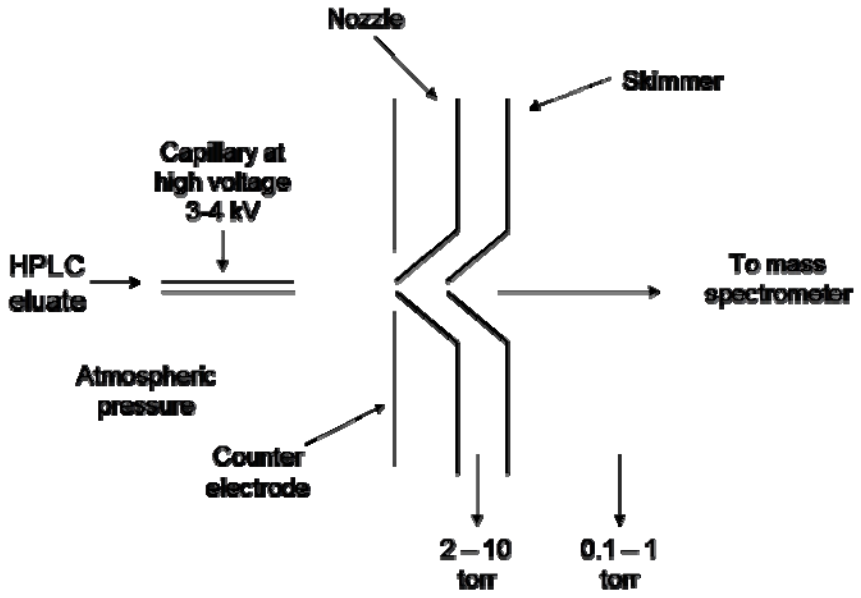

Figure 2.4. Schematic of an electrospray LC-MS interface (*35*).

2.3. MASS SPECTROMETRY

Mass spectrometry involves three steps: ionization of the analyte, mass separation of the ions, and detection of ions. There are many types of mass spectrometers that are used today, but in our studies, a quadrupole tandem mass spectrometer was used. A quadrupole mass spectrometer guides ions to the detector by separating them based on their mass to charge ratio (m/z) by d.c. and oscillating r.f. voltages. Only ions that are stable in the r.f. and d.c voltages reach the detector. Further details can be found in (*33,35,37*).

2.3.1. TANDEM MASS SPECTROMETRY

Tandem mass spectrometry can indicate molecular weight as well as structural information of the analyte *(35)*. It has three quadrupole mass filters which improves selectivity and sensitivity. Quads one (Q1) and three (Q3) are for scanning, while quad two (Q2) is the collision cell (figure 2.6). Ions enter Q1 and selected ions, the precursor ions, are isolated based on the voltage of the quadrupole (*33,35*). The precursor ions then enter Q2, which has r.f. only and is at a high pressure. Due to the high pressure, the ions have low energy collisions with the background nitrogen gas (*33,35*). Some of the kinetic energy from the incoming ions is converted to internal energy, which results in uni-molecular decompositions of the ions producing fragments from the precursor ions (*33*). The fragments, or product ions are focused into Q3 where selected ions are mass analyzed. A signal is only seen when the ion passes through all three quads.

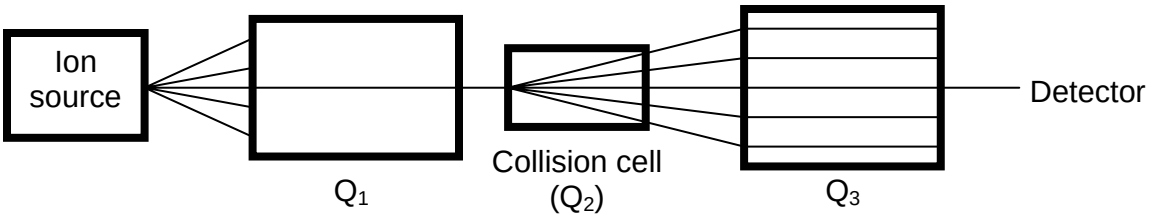

Figure 2.5. Schematic of tandem MS/MS quadrupole mass spectrometer *(35)*.

There is a continuous stream of ions that flows from the ion source to the detector with a transit time of ~50-100 microseconds (*33*). When the ions enter the detector, they produce a signal that is equivalent to the abundance of ions that enters it.

Chapter 3

EXPERIMENTAL

3.1. CHEMICALS

Native, $^{13}C_{12}$- and d_{18}-labeled α–, β– and γ–HBCD (99.8%) were obtained from Wellington Laboratories (Guelph, ON, Canada). HPLC optima grade methanol and water were obtained from Fisher Scientific (Nepean, ON, Canada). Distilled in glass hexane, dichloromethane (DCM) and acetone were obtained from Caledon (Edmonton, AB, Canada). Corn oil, gelatin, and tricaine methanesulfonate (MS 222) were purchased from Sigma-Aldrich (Oakville, ON, Canada). Ottawa sand (20-30 mesh) was obtained from Fisher Scientific (ON, Canada)

A labelled recovery internal standard (LRIS; 5 ng of $^{13}C_{12}$ α–, β–, and γ–HBCD) was added to each sample to correct for recovery of the individual isomers. A labelled instrument performance matrix internal standard (LIPMIS; 5 ng of d_{18} α–, β–, and γ–HBCD) was added to the extract prior to being run on the LC/MS/MS to correct for instrument performance and matrix effects.

3.2. HIGH PERFORMANCE LIQUID CHROMATOGRAPHY

HPLC separations were done on an Agilent 1100 series HPLC system (Agilent Technologies, Palo Alto, CA, USA) equipped with a vacuum degasser, binary pump and an autosampler was used. A Genesis C_{18} analytical column (10 cm × 2.1 mm i.d., 4 μm particle size; Jones Chromatography, Chromatographic Specialties Inc., Brockville, ON, Canada) was used on all samples. A mobile phase of optima grade water and optima grade methanol at a flow-rate of 300 μL/min was used. The elution program started at an initial composition of 30:70 water/MeOH (v/v) and was ramped linearly to 100% MeOH in 3 minutes. This was held for 3.5 min and then returned to starting conditions in 3 minutes. The column was allowed to equilibrate for 6 minutes between runs (*28*).

3.3. GAS CHROMATOGRAPHY

All analyses were performed on an Agilent 5973 GC-MSD fitted with a 10m × 0.25 μm i.d. (0.25 μm film thickness) DB-5 capillary column (J&W Scientific, CA). UHP helium was used as the carrier gas. Splitless injections of 2 μL were made by a 7683 Agilent autosampler with the injector set isothermally at 260 ºC. The initial oven temperature was set at 90 ºC with no hold time, ramped at 20 ºC/min to 250 ºC with no hold time, and ramped at 5 ºC/min to 300 ºC and held for 22min.

3.4. MASS SPECTROMETRY

A Sciex API 2000 triple quadrupole mass spectrometer (Applied Biosystems, Foster City, CA, USA) was used in the ESI negative ion mode. Quantitation was achieved by monitoring the specific $[M\text{-}H]^-$ ($C_{12}H_{17}{}^{79}Br_3{}^{81}Br_3$, *m/z* 640.6) $\rightarrow Br^-$ (*m/z* 79 and 81) multiple reaction monitoring (MRM) ion transition. MS/MS detection of d_{18}–HBCD and $^{13}C_{12}$–HBCD isomers was based on the analogous ($[M - H]^-$) $\rightarrow Br^-$ reaction monitored for the native HBCD (*m/z* d_{18}: 657.6 and $^{13}C_{12}$: 652.4 ($[M - H]^-$)). Detection utilized unit resolution on the first and third quadrupoles and a 200ms dwell time. Collision activated dissociation gas pressure was 8 a.u. and the collision energy was 50eV. Additional source parameters are given in Table 3.1. Our instrument sensitivity was improved with a recent upgrade to the collision cell (mSpec Corporation, ON, Canada) (*28*). All gas supplies were provided from a nitrogen generator (Peak Scientific, Renfrewshire, Scotland, UK).

Table 3.1. Parameter of MS/MS (*28*)

Parameter	Abbreviation	Value (units)
Curtain gas	CUR	25 (a.u.)
Sheath gas	GS1	35 (a.u.)
Turbo gas	GS2	30 (a.u.)
Ionspray voltage	IS	-4000 (V)
Turbo-gas temperature	TEM	500 (°C)
Declustering potential	DP	-5.0 (V)
Focusing potential	FP	-360 (V)
Entrance potential	EP	-4.5 (V)
Quad 1 offset	IQ1	11.0 (V)
Prefilter (stubbies)	ST	19.5 (V)
Collision gas	CAD	8 (a.u.)
Collision cell entrance potential	CEP	51.0 (V)
Collision energy	CE	50 (eV)
Collision cell exit potential	CXP	-5.0 (V)

3.5. QUALITY ASSURANCE/QUALITY CONTROL

Instrument blanks were injections of methanol run after every 5 samples and were used to monitor HBCD contamination between HPLC injections. Extraction blanks were derived by extraction of control fish muscle tissue and also extraction of Na_2SO_4. Extraction blanks were used to monitor the potential for contamination to occur during extraction and work-up of the sample.

Method detection limits (MDLs) were determined by spiking known amounts of the native HBCD isomers into muscle tissue extracts of the control fish (*n=4*) that were previously analyzed and found to have non-detectable concentrations of the isomers, *i.e.*, response of isomers were not above the response from the extraction blanks. Five separate injections of the spiked extracts were then made. The ion signals obtained for the three isomers were then adjusted to estimate concentrations that would give a signal-

to-noise ratio of 3:1. In this manner, MDLs of the three isomers were estimated to be 0.01 ng/g. For calculation of mean concentrations and for statistical purposes, a concentration of ½ of the MDLs was assumed in those instances where the isomers were below MDLs.

3.6. FOOD PREPARATION

Commercial starter fish food (~1.5 ± 0.2 Kg of Silver Cod; Martin's Feed Mills, Elmira, ON, Canada) was added to a pre-cleaned (soap and water, then rinsed with methanol) Hobart blender. Corn oil (20 mLs) was added to the feed then mixed for ~20 minutes. A gelatin binder was prepared by vigorously stirring 40 g of gelatin (Sigma-Aldrich; Oakville, ON, Canada) to 1.5 L of Milli- Q water (heated to 30-37°C). The aqueous gelatin was slowly incorporated into the food and mixed until the food had a firm consistency (~20 minutes). The fish food was air dried for 1 hour, and then was extruded (4 mm diameter) using a meat grinder. Food was then thoroughly dried at 25°C for 2-3 days. Fish food was then crushed into pellets. Four batches of food were prepared in this study (all prepared as above): three of the batches were spiked with a known amount of an individual native diastereoisomer (α–, β– or γ–HBCD) which was added into the corn oil, while no diastereoisomer was added to the fourth batch (control fish food).

The lipid content of food (±SE, n=4) were determined gravimetrically (see equation [3-1], page 48) and were found to be: α (10.81 ± 0.76%); β (12.52 ± 0.52%); γ (14.12 ± 0.25%) and control (14.43 ± 0.14%). Non-lipid corrected concentrations of the isomers in the food were determined to be: α (7.26 ± 4.17ng/g); β (6.01 ± 3.73ng/g); γ (5.5 ±

3.00ng/g). Concentrations were normalized to lipid content by dividing wet? weight concentrations by lipid content and found to be: α (29.14 ± 1.95 ng/g); β (11.84 ± 1.95 ng/g); γ (22.84 ± 2.26 ng/g). Respective lipid normalized concentrations of α– and γ–HBCD in the control food were 0.07 and 0.30 ng/g; the β–isomer was below method detection limits. Food was stored in the dark at –4°C to limit the possibility of photo transformations.

3.7. EXPOSURE EXPERIMENT

Juvenile rainbow trout were individually weighed and randomly separated into four 800L fibreglass aquaria (the initial mean weight of all the fish was 233 $\pm$ 89 g). Each tank received water at a constant water flow of 1.5 L/min of UV- and carbon-dechlorinated Winnipeg City tap water, at a temperature of 11-12°C and pH between 7.9 and 9.1. The dissolved oxygen was always at level of saturation. A 12-h light 12-h dark photoperiod was maintained throughout the experiment. Fish were acclimatized in their respective tanks for 7 days prior to the start of the experiment and fed the control food. Fish in each of the three tanks were exposed to an individual HBCD isomer *via* their food; fish in the fourth tank were exposed to control food (i.e., unfortified food) throughout the experiment. There was an uptake phase of 56 days, where fish were fed fortified food, followed by a depuration phase of 112 days, where all fish were fed unfortified food. The feeding rate was 1% of their body weight three times a week. This rate was adjusted after each sampling day based on the mean weight of the fish sacrificed, and on the reduction of the number of fish in tank, as described below. Four fish from each tank

were sacrificed on days 0, 7, 14, and 56 of the uptake phase and days 7, 14, 56, and 112 of the depuration phase. Fish were sacrificed 48 hours after the previous feeding by an overdose of a pH buffered solution of MS-222 (0.4 g/L). Once operculum movement ceased (<3 min) 3-5 mL of blood was removed *via* the caudal vein with a heparinized syringe, along with the liver, kidney, muscle tissue and thyroid. Whole fish and their various parts were weighed. Details of the handling of samples for biochemical analysis (not part of this thesis) can be found in Palace *et al*. (*38*). Only muscle tissue from the carcass was used for calculating bioaccumulation parameters whereas liver and muscle tissue were used for screening for phase I cytochrome P450 enzyme activities (not described) and debromination metabolites.

3.8. SAMPLE EXTRACTION

Muscle tissue samples were dry ice homogenized and weighed prior to extraction (see figure 3.1). A Dionex accelerated solvent extractor 300 (ASE) (Dionex Canada Ltd., Oakville, ON, Canada) was used to extract HBCD from the muscle tissue. Weighed samples (~15 g) were mixed with heat-treated (600^{o}C for 6h) pelleted diatomaceous earth and added to the 100 mL ASE cell. Cells were spiked with 10 µL of a 500 ng/µL $^{13}C_{12}$ α–, β–, γ–HBCD LRIS solution. Heat treated (600^{o}C for 6h) Ottawa sand was added to fill any voids. The ASE parameters were as follows; solvent 50:50 DCM:hexane; temperature 125°C; pressure 1500 psi; heat-up time 6 min; static time 5 min; flush volume 60%; purge time 120 s; static cycles 2 (*31*). The organic extracts were then dried over heat treated (600^{o}C for 6h) anhydrous sodium sulfate (10-60 mesh size), reduced in volume to 8 ml, and filtered (1 µm PTFE syringe filters, Gelman Laboratory, MI). An

aliquot (1 mL) of each extract was added to an aluminium foil weigh boat, weighed, evaporated to dryness and weighed again. Lipid weights were determined gravimetrically using equation 3-1.

$$\%\ \text{lipid} = \left[\frac{\left(\left(weight\ of\ weigh\ boat + lipid \right) - weight\ of\ weigh\ boat \right) \times 8}{weight\ of\ sample} \right] \times 100 \quad [3\text{-}1]$$

Lipid was removed from the remaining extract by using an automated gel permeation chromatograph (J2 Scientific, Columbia, Missouri, USA) on a column (29.5 mm i.d x 400 mm) packed with 60 g (dry weight) of 200-400 mesh S-X3 Envirobeads (ABC Instruments, MO) that had been soaked in DCM/hexane overnight. Further purification was achieved on a column (300 mm x 10.5 mm i.d.) of reagent-grade Florisil (1.2% deactivated (w/w), 8 g, 60-100 mesh size, Fisher Scientific). HBCD was eluted off the column using 35 mL of hexane:DCM (85:15) followed by 50 mL of hexane:DCM (50:50). The collected fraction was reduced in volume to 200 µL by a gentle stream of ultra high purity N_2 and spiked with 10 µL of 500 ng/µL d_{18} α–, β–, γ–HBCD LIPMIS prior to liquid chromatography tandem mass spectrometry analysis (LC/MS/MS).

To check for metabolites of HBCD, livers were extracted by ball-milling with 70:30 hexane/acetone. Extracts were treated in an identical manner to the tissue extracts except that the addition of internal standards and the Florisil step were both omitted; hydroxylated HBCD (OH-HBCD) metabolites may be retained on the adsorbent material.

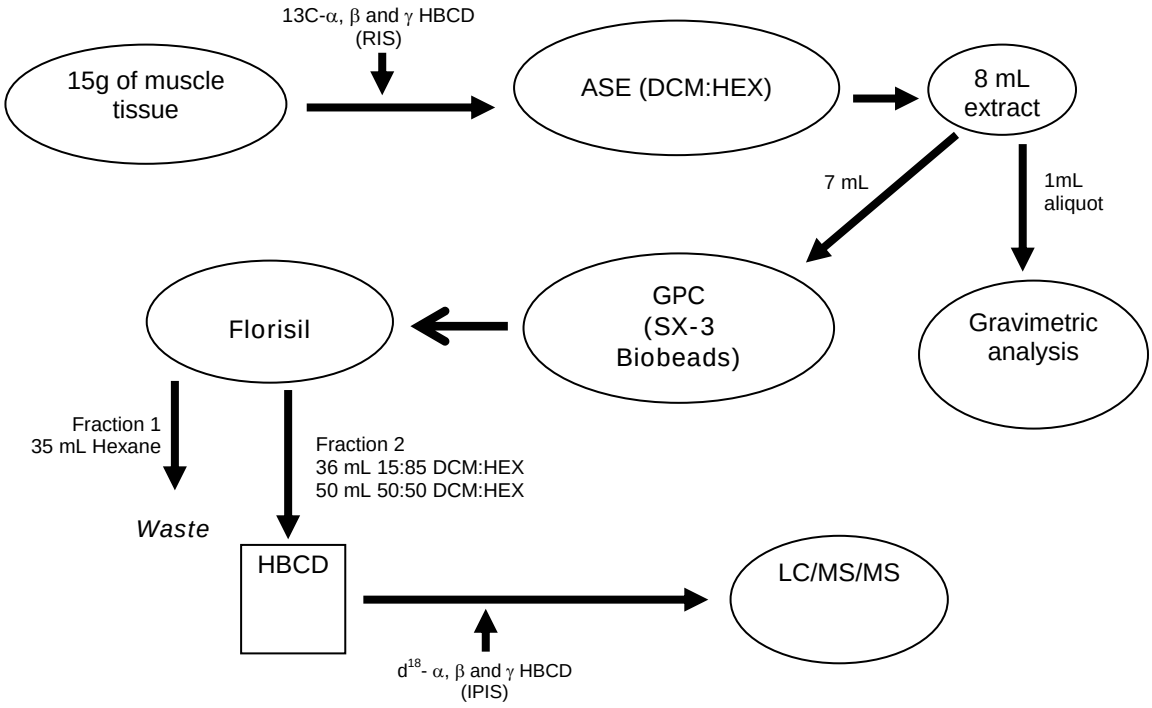

Figure 3.1. Schematic of HBCD extraction from fish tissue.

3.9. DATA ANALYSIS

Concentrations of each diastereoisomer in muscle tissue of the control fish were subtracted from the concentrations of respective diastereoisomer in the muscle tissue of the fish exposed to the fortified food. Correction for growth dilution and lipid content is common in modelling the bioaccumulation of contaminants in the laboratory. Diastereoisomeric concentrations in the fish exposed to the fortified food were also corrected for recovery of the ^{13}C recovery internal standard.

3.9.1. STATISTICAL ANALYSIS

Regression analysis was done using Systat SigmaPlot 2001 and student t-test were determined using Microsoft Excel. The statistical Q-test was the criterion used for rejection or retention of outliers (*39*).

Chapter 4

RESULTS AND DISSCUSION

4.1 GROWTH RATES

Fish growth rates were estimated by plotting the ratio of the average weight of fish at each sampling point (W_t) to the average fish weight at the start of the experiment (W_0 = 233g) versus time (Figure 4.1a-d). Regression analysis suggests that fish are growing linearly throughout our study time period. Respective growth rates (d^{-1}), derived from the slope of the plots, for fish in the four treatment tanks were α: 0.0074; β: 0.0067; γ: 0.0054 and control: 0.0048 per day.

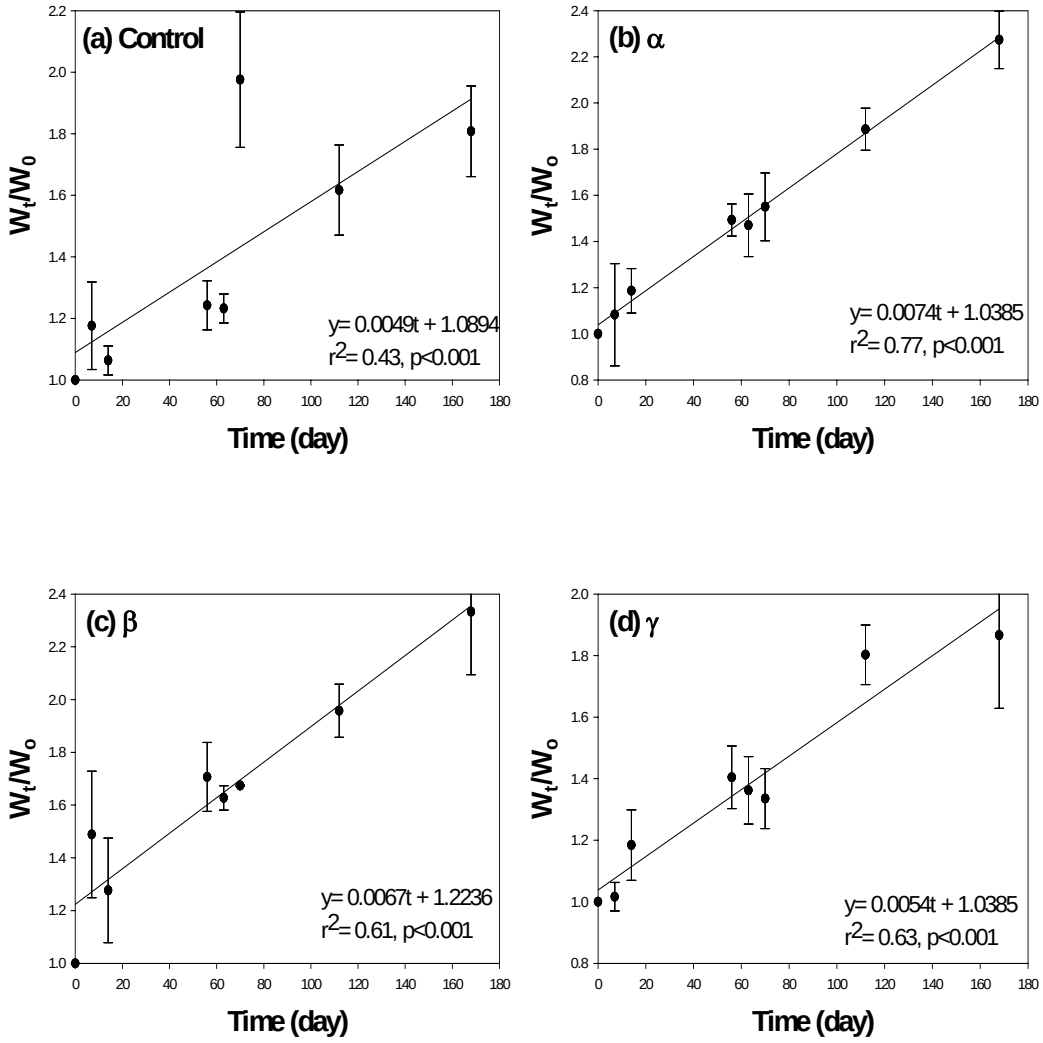

Figure 4.1. Plots showing the growth rates of juvenile rainbow trout exposed to food fortified with (a) control (no isomer added) (b) α– (c) β– and (d) γ–HBCD. Results of linear regression analysis shown in each plot. Each data point represents the mean of four fish.

4.2 DIASTEREOISOMERIC AMOUNTS

Tables 4.1 and 4.2 show the average nmoles of each diastereoisomer in the muscle tissue during the uptake and depuration phases. Table 4.3 shows the same data but expressed in concentration (ng/g). All calculations preformed in this thesis that required a mass value, were based on the mean muscle tissue sampled (Table 4.3) as this allowed us to compare data that had a known measured amount of muscle tissue.

Table 4.1. Average nmoles ± 1 standard error of each diastereoisomer in muscle tissue on each sacrifice day during the uptake phase.

Isomer fed to fish	Day 0			Day 7			Day 14			Day 56		
	α	β	γ	α	β	γ	α	β	γ	α	β	γ
α-fish	0.06 ± 0.04	<MDL	0.08 ± 0.04	0.06 ± 0.02	<MDL	0.01 ± 0.005	0.15 ± 0.009	<MDL	0.06 ± 0.03	0.89 ± 0.2	0.09 ± 0.04	0.12 ± 0.07
β-fish	0.01 ± 0.005	0.04 ± 0.02	0.01 ± 0.004	0.02 ± 0.01	0.07 ± 0.01	0.06 ± 0.04	0.02 ± 0.01	0.09 ± 0.01	<MDL	0.02 ± 0.01	0.31 ± 0.06	0.29 ± 0.25
γ-fish	<MDL	0.009 ± 0.02	0.05 ± 0.02	0.06 ± 0.02	0.01 ± 0.005	0.12 ± 0.02	0.04 ± 0.02	<MDL	0.34 ± 0.2	<MDL	<MDL	0.21 ± 0.07

All nmoles are control and lipid corrected

Table 4.2. Average nmoles ± 1 standard error of each diastereoisomer in muscle tissue on each sacrifice day during the depuration phase.

Isomer fed to fish	Day 63			Day 70			Day 112			Day 168		
	α	β	γ	α	β	γ	α	β	γ	α	β	γ
α-fish	0.25± 0.06	0.008 ± 0.002	<MDL	0.26 ± 0.12	0.03 ± 0.01	0.06 ± 0.03	0.34 ± 0.11	0.02 ± 0.006	0.10 ± 0.05	0.26 ± 0.05	<MDL	0.03 ± 0.009
β-fish	<MDL	0.33 ± 0.14	<MDL	<MDL	0.29 ± 0.08	0.08 ± 0.003	0.005 ± 0.003	0.14 ± 0.07	0.06 ± 0.03	0.16 ± 0.03	0.14 ± 0.04	0.06 ± 0.01
γ-fish	0.05 ± 0.03	<MDL	0.26 ± 0.05	0.15 ± 0.10	0.03 ± 0.02	0.15 ± 0.03	0.05 ± 0.03	<MDL	0.13 ± 0.05	0.11 ± 0.02	<MDL	0.09 ± 0.006

All nmoles are control and lipid corrected

Table 4.3. Mean lipid (%), whole fish weight (g), muscle tissue used (g), fork length (cm) and concentration (ng/g)[a] ± 1 standard error of each diastereoisomer in muscle tissue on each sacrifice day during the uptake phase.

Day	Mean Lipid (%)	Mean whole fish weight (g)	Mean Muscle tissue sampled (g)	Mean fork length (cm)	α-isomer fed fish[a]			β-isomer fed fish[a]			γ-isomer fed fish[a]		
					α-isomer	β-isomer	γ-isomer	α-isomer	β-isomer	γ-isomer	α-isomer	β-isomer	γ-isomer
0	1.51 ± 0.23	233.4 ± 10.4	15.03 ± 0.02	27.3 ± 0.04	2.76 ± 1.56	<MDL	3.80 ± 1.88	0.62 ± 0.27	1.86 ± 0.98	0.41 ± 0.31	<MDL	0.38 ± 0.24	2.55 ± 0.68
7	1.64 ± 0.23	249.5 ± 19.4	15.03 ± 0.02	27.8 ± 0.6	2.38 ± 1.07	<MDL	0.31 ± 0.30	0.85 ± 0.52	3.06 ± 0.53	2.47 ± 1.75	2.36 ± 0.92	0.45 ± 0.32	5.02 ± 0.92
14	1.25 ± 0.10	2.46.7 ± 12.5	15.03 ± 0.03	27.7± 0.3	6.55 ± 0.38	<MDL	1.72 ± 0.99	0.88 ± 0.45	4.17 ± 0.50	<MDL	1.55 ± 1.02	<MDL	13.15 ± 8.48
56	0.94 ± 0.13	306.2 ± 12.9	15.04± 0.03	29.5 ± 0.4	37.85 ± 7.10	3.80 ± 1.90	4.85 ± 3.24	0.70 ± 0.69	13.21 ± 2.59	1.64 ± 1.63	<MDL	<MDL	9.19 ± 3.10

[a]Values are control and lipid corrected.

Table 4.4. Mean lipid (%), whole fish weight (g), muscle tissue used (g), fork length (cm) and concentration (ng/g)[a] ± 1 standard error of each diastereoisomer in muscle tissue on each sacrifice day during the depuration phase.

Day	Mean Lipid (%)	Mean whole fish weight (g)	Mean Muscle tissue sampled (g)	Mean fork length (cm)	α-isomer fed fish[a]			β-isomer fed fish[a]			γ-isomer fed fish[a]		
					α-isomer	β-isomer	γ-isomer	α-isomer	β-isomer	γ-isomer	α-isomer	β-isomer	γ-isomer
56	0.94 ± 0.13	306.2 ± 12.9	15.04± 0.03	29.5 ± 0.4	37.85 ± 7.10	3.80 ± 1.90	4.85 ± 3.24	0.70 ± 0.69	13.21 ± 2.59	1.64 ± 1.63	<MDL	<MDL	9.19 ± 3.10
63	0.85± 0.12	292.0 ± 12.4	15.03 ± 0.03	28.8 ± 0.4	11.02 ± 0.87	0.23 ± 0.15	<MDL	<MDL	14.15 ± 6.23	<MDL	0.77 ± 0.67	<MDL	11.10 ± 2.00
70	0.87 ± 0.11	341.1 ± 20.9	15.03 ± 0.02	30.5± 0.6	13.31 ± 5.04	1.05 ± 0.64	1.82 ± 1.28	<MDL	0.29 ± 0.08	2.42 ± 0.002	8.03 ± 4.58	1.31 ± 0.93	5.18 ± 1.43
112	1.01± 0.15	378.4 ± 12.7	15.03± 0.03	31.6 ± 0.4	14.35 ± 4.90	0.02 ± 0.006	4.10 ± 2.08	0.12 ± 0.04	0.14 ± 0.07	2.69 ± 1.41	2.01 ± 1.36	<MDL	5.77 ± 2.06
168	0.64 ± 0.09	433.7 ± 22.2	15.04 ± 0.03	33.3± 0.6	7.59 ± 2.21	<MDL	1.42 ± 0.39	3.34 ± 1.27	5.23 ± 1.51	2.85 ± 0.56	0.74 ± 0.73	<MDL	3.97 ± 0.25

[a]Values are control and lipid corrected.

4.3 BIOACCUMULATION

The appearance of the uptake plots (Figures 4.4-4.6) suggests that the diastereoisomers that were exposed to the fish via their diet were detectable in the muscle tissue after 7 days of exposure. To test whether uptake into the muscle tissue followed a first order rate process, the number of nmoles in the muscle tissue at each time point was logarithmically transformed then the average was taken and plotted against time [Figure 4.2(a)-(c)].

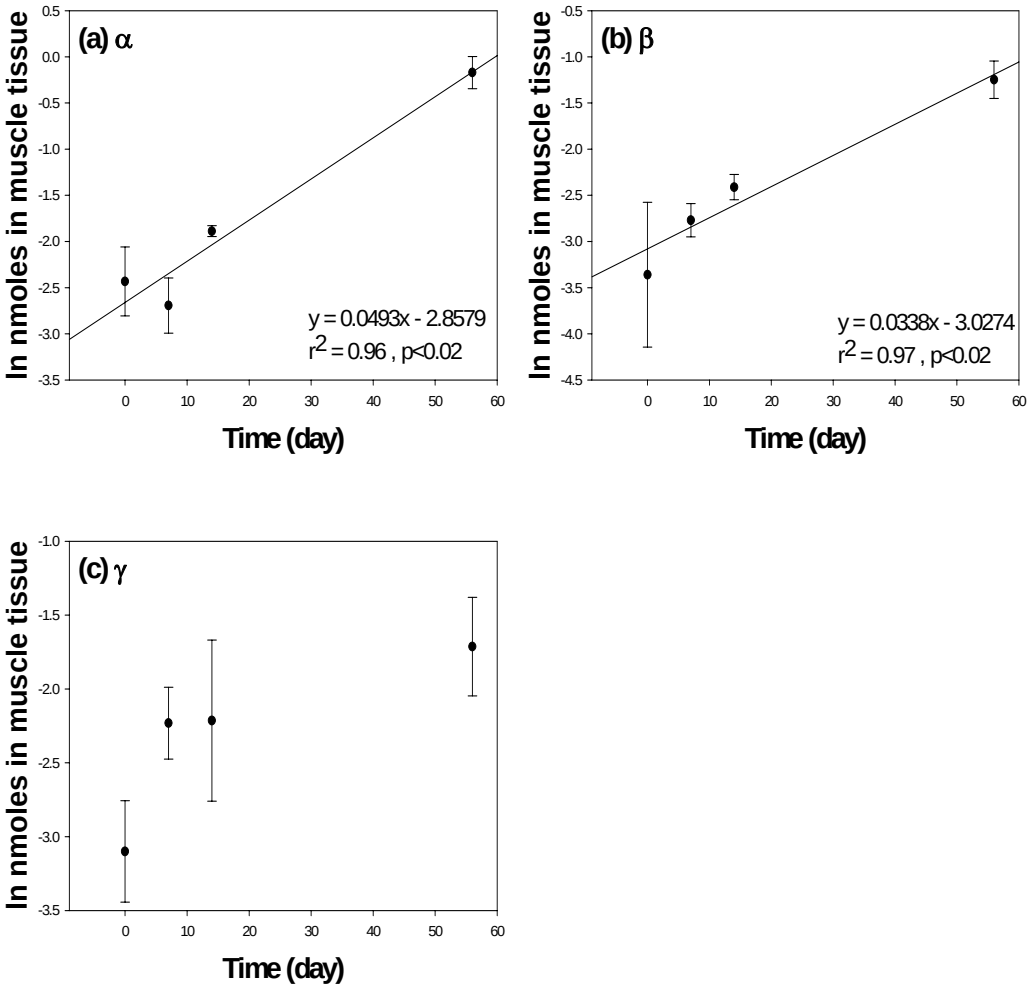

Figure 4.2. Plots of logarithmically transformed nmoles in muscle tissue versus time (days) for fish exposed to (a) α- (b) β- and (c) γ-isomer during the uptake phase. Regression analysis shown in plots (a) and (b). Each data point represents the mean of four fish.

The plots shown in Figure 4.2 suggest that both the α– (r^2=0.96, p<0.02) and β–isomers (r^2=0.97, p<0.02) are increasing exponentially in the fish during the uptake phase of the experiment. Doubling times (d_t, days), calculated by using the equation;

$$d_t = \frac{\ln 2}{exponential\,uptake} \quad [4\text{-}2]$$

were found to be 14.1 $\pm$ 1.4 and 20.5 $\pm$ 4.9 days for the α– and β–isomers, respectively.

Figure 4.2 (c) suggest that the uptake of the γ-isomer into the muscle tissue did not follow a first order uptake process. In fact, the uptake of this isomer was found to increase linearly (r^2=0.84, p<0.06) during the uptake phase of our experiment (plot not shown). None of the diastereoisomers reached steady-state within the 56-day uptake phase (Figure 4.4-4.6).

4.4 DEPURATION

The depuration of the α–diastereoisomer (Figure 4.4) showed an initial rapid depuration for the first 14 days followed by a slower depuration rate over the remainder of the experiment. Both the β– (Figure 4.5) and the γ–diastereoisomers (Figure 4.6) were still accumulating after the first 7 days of exposure to control food; beyond that time, they began to slowly depurate from the fish. It remains unclear why accumulation was still occurring but perhaps assimilation of both β– and γ–diastereoisomers from the gut was slower than that of the α–diastereoisomer.

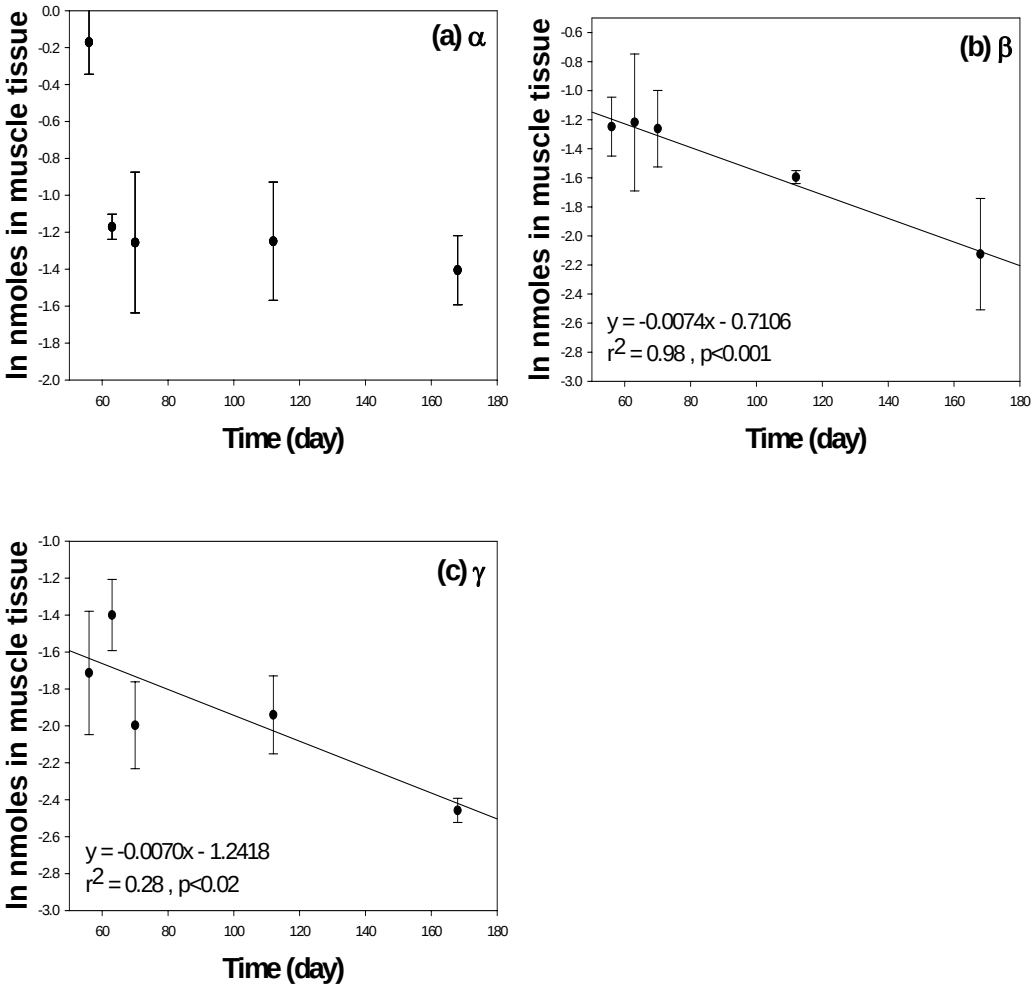

Figure 4.3. P lots of logarithmically transformed nmoles in muscle tissue versus time (days) for fish exposed to (a) α- (b) β- and (c) γ-isomer during the clearance phase. Regression analysis shown in plots (b) and (c). Each data point represents the mean of four fish.

To test whether clearance from the muscle tissue followed a first order rate process, the number of nmoles in the muscle tissue at each time point was logarithmically transformed then the average was taken and plotted against time [Figure 4.3(a)-(c)]. The plots shown in Figure 4.3 suggest that both the β– and γ–isomers are decreasing exponentially in the fish during the clearance phase of the experiment. Calculated depuration rate constants (k_d = slope of natural log of the number of nmoles versus time) were 0.74×10^{-2} d^{-1} (r^2= 0.98, p=0.001) and 0.83×10^{-2} d^{-1} (r^2=0.82, p=0.02) for the β– and γ–isomers, respectively (Table 4.1). The depuration half lives ($t_{1/2}$, days) of β– and γ–isomers calculated by using the equation:

$$t_{1/2} = \frac{\ln(2)}{k_d} \quad [4\text{-}3]$$

were 94 ± 25 and 84 ± 51 days, respectively. No kinetic information could be gleaned for the α–isomer because depuration out of the muscle tissue did not obey a first order rate process.

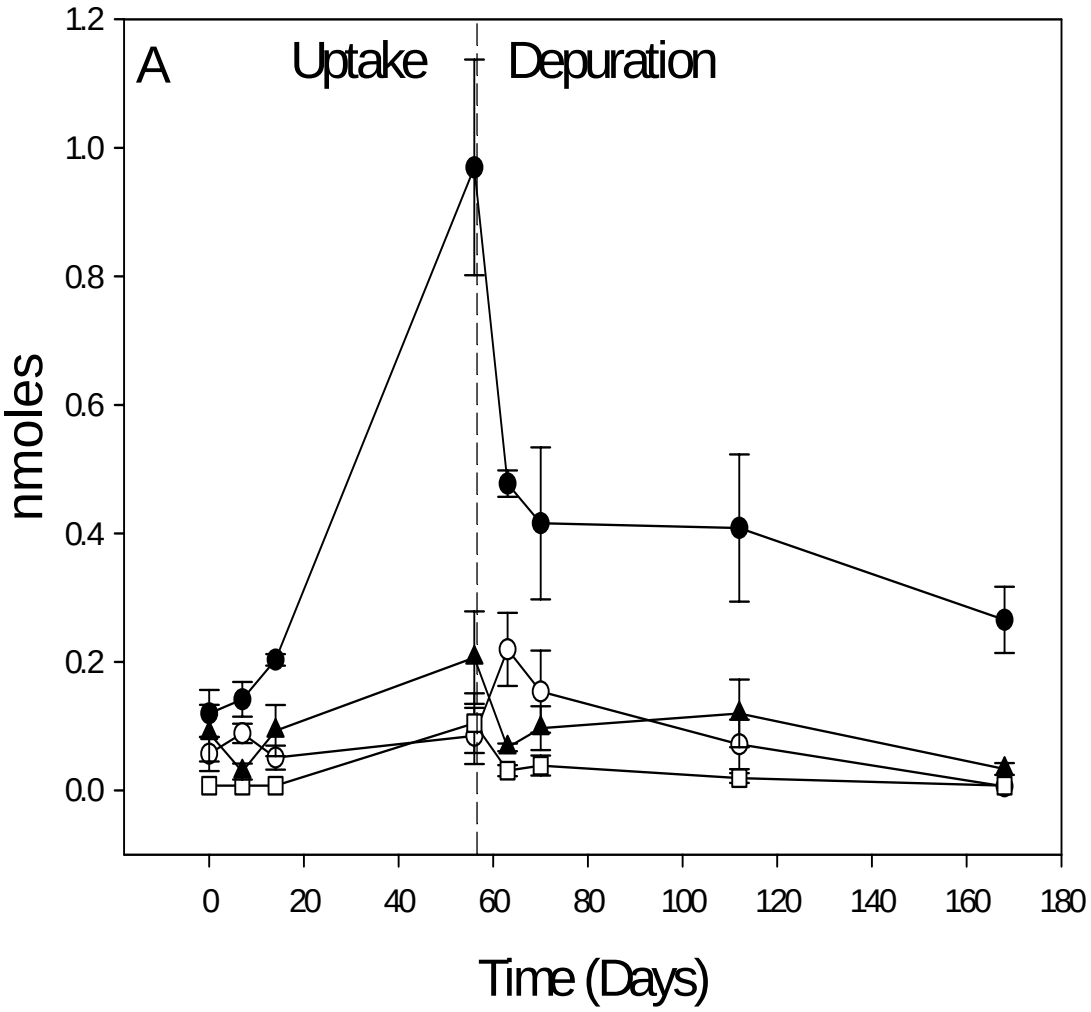

Figure 4.4. Uptake and depuration of juvenile rainbow trout exposed to α-HBCD. Each point (control (o), α- (●), β- (□), and γ- (▲) diastereoisomers) is the mean ± 1 standard error (vertical bars) of four fish. Molar amounts are for muscle tissue, corrected for growth dilution and lipid content. Control fish were analyzed for each individual diastereoisomer.

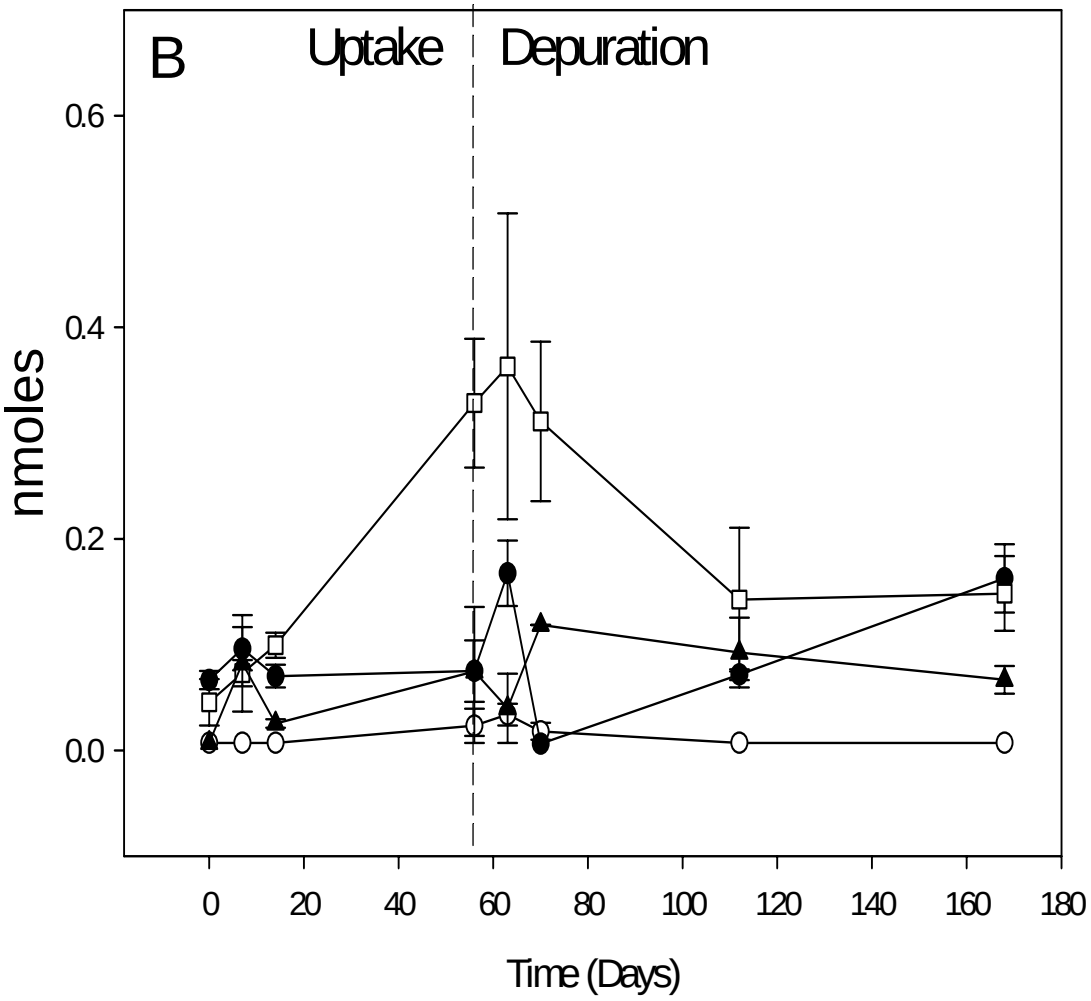

Figure 4.5. Uptake and depuration of juvenile rainbow trout exposed to β-HBCD. Each point (control (o), α- (●), β- (□), and γ- (▲)diastereoisomers) is the mean ± 1 standard error (vertical bars) of four fish. Molar amounts are for muscle tissue, corrected for growth dilution and lipid content. Control fish were analyzed for each individual diastereoisomer.

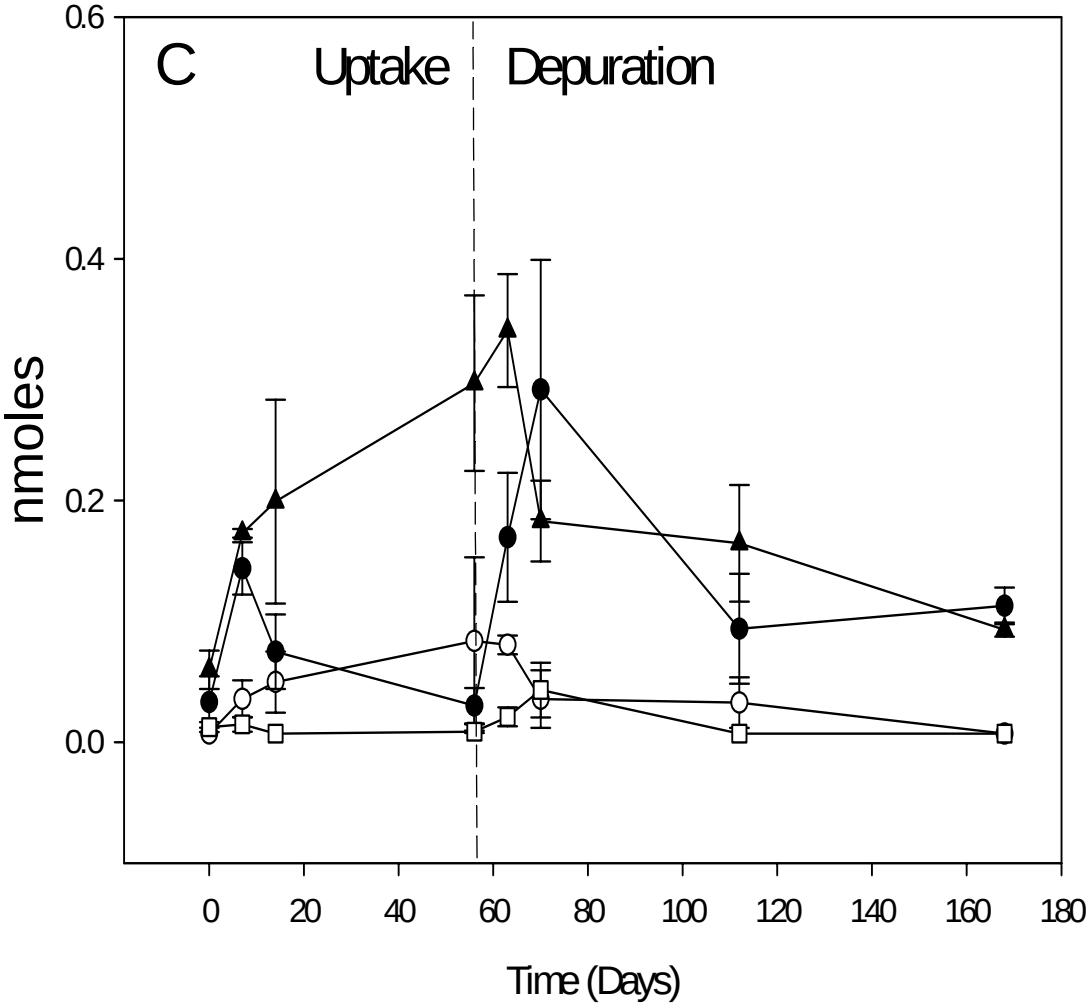

Figure 4.6. Uptake and depuration of juvenile rainbow trout exposed to γ-HBCD. Each point (control (o), α- (●), β- (□), and γ- (▲)diastereoisomers) is the mean ± 1 standard error (vertical bars) of four fish. Molar amounts are for muscle tissue, corrected for growth dilution and lipid content. Control fish were analyzed for each individual diastereoisomer.

4.5 BIOACCUMULATION PARAMETERS

Table 4.3 synthesizes bioaccumulation parameters of the individual isomers.

Assimilation efficiencies (AE; shown in Table 4.4) were calculated using the following equation from Tomy *et al*. (*31*);

$$AE = \frac{(control\,corrected\ concentration\ \ in\ \ fish)\times(mass\ of\ \ fish\ muscle)}{(control\ \ concentration\ in\ \ food)\times(mass\ of\ \ food\ \ eaten)} \quad [4\text{-}4]$$

A biomagnification factor (BMF) is the magnification of concentration of the contaminent in an organisms lipid relative to its concentration in the food. The BMFs were calculated from the equation:

$$BMF = \frac{AE \times F}{k_d} \quad [4\text{-}5]$$

where the feeding rate (F) for α–, β–, and γ–isomers were equal to 6.75, 4.55, and 7.44% of the body weight of the fish per day, respectively and k_d is the first order depuration rate constant.

Another equation used to calculate BMF is as follows;

$$BMF = \frac{[HBCD]_{in\ the\ predator}}{[HBCD]_{in\ the\ prey}} \quad [4\text{-}6]$$

where the numerator is the mean concentration of HBCD in the fish at day 56 and the denominator is the accumulated concentration of HBCD that fish were exposed over 56 days. This simplified equation must be used with some caution as it assumes that fish consume 100% of the food and that the food is evenly distributed amongst the fish.

Table 4.5. Bioaccumulation parameters of HBCD diastereoisomers from dietary exposures using juvenile rainbow trout.

	Depuration rate constant[a] (k_d) x 10^{-2} (d^{-1})	Half-life[b] ($t_{1/2}$) (d)	Average AE (%)	BMF 1[c]	BMF 2[d]
α–HBCD	nd	nd	28.4	4.3	1.3
β–HBCD	0.74 ± 0.2	94 ± 25	36.4	2.6	1.1
γ–HBCD	0.83 ± 0.5	84 ± 51	34.2	3.6	0.40

[a]Depuration rate constants (k_d) (±1 standard error) were calculated using the model ln concentration (lipid weight basis) = a + b(time) Coefficient of determination shown for the model shown in parentheses; [b]Half-life (± standard error) calculated from the equation $t_{1/2}=0.693/k_d$; no half life for α-HBCD was calculated (see text for details); [c]Biomagnification factors (BMFs) were calculated from the equation BMF= (AE × F)/k_d, where F is the feeding rate on a lipid basis and k_d is the depuration rate constant and AE is the assimilation efficiency; [d] BMF calculated from the equation BMF= $[HBCD]_{in\ the\ predator}$/ $[HBCD]_{in\ the\ prey}$

4.6. BIOLOGICAL EFFECTS

The growth rates of the control fish compared to the fish exposed to the α– and β–fortified food varied and was found to be statistically different ($p<0.05$ and $p<0.02$, respectively). This suggests that α– and β–HBCD increases the rate of growth. γ–HBCD did not affect the rate of growth of the rainbow trout. The percent lipid increased in the α–HBCD fed fish from the end of the uptake phase to the end of the depuration phase and decreased in all other treatments, including the control (Table 4.5). No mortalities occurred throughout this experiment. A more detailed study on biochemical effects is the focus of another study (*38*).

Table 4.6. Growth parameters in body and liver, mortality and liver somatic index of juvenile rainbow trout exposed to HBCD isomers.

	Growth rate[a]	% lipid[b]		Liver somatic index[c] (%)		
treatment	Whole fish $\times 10^{-3}$ (d^{-1})	Day 56	Day 168	Day 56	Day 168	Mortality (*22*)
Control	4.8 (0.43)	0.90± 0.24	0.33 ± 0.12	0.77 ± 0.04	0.63 ± 0.02	0
α–HBCD	7.4 (0.77)	0.51± 0.06	0.82 ± 0.15	0.75 ± 0.02	0.68 ± 0.03	0
β–HBCD	6.7 (0.61)	1.17± 0.12	0.69 ± 0.06	0.85 ± 0.03	0.72 ± 0.07	0
γ–HBCD	4.8 (0.63)	1.18± 0.15	0.70 ± 0.33	0.77 ± 0.05	0.82 ± 0.06	0

[a]Growth rates were calculated by $W_t=W_o$ [1+ b x time (d)], where b is the growth rate (coefficient of determination for the model is shown in parentheses); [b]% lipid is an average (± standard error) of the fish (*n=4*) samples on that day; [c]liver somatic index (± standard error) calculated as (liver weight ÷whole fish weight) x 100.

4.7. BIOISOMERIZATION

At day 168 of depuration, fish exposed exclusively to the β–diastereoisomer show statistically significant molar amounts of the α–diastereoisomer ($p<0.002$) and γ–diastereoisomer ($p=0.01$) compared to the controls. The fact that the β–diastereoisomer can bioisomerize and that it is detected at relatively small amounts in commercial mixtures partly explains why it is present at small concentrations in biota. The α–diastereoisomer was also observed in fish exposed exclusively to the γ–diastereoisomer (Figure 4.6): at day 168, statistically significant ($p<0.004$) molar amounts of the α–diastereoisomer were found in fish (Table 4.6). Taken together, these findings strongly suggest that juvenile rainbow trout have the capability to bioisomerize the β– and γ–diastereoisomers of HBCD. The α–diastereoisomer appears to be recalcitrant to bioisomerization in this particular fish species.

Trace quantities of the α– and γ–diastereoisomers were detectable in control food. It could be argued that the presence of these diastereoisomers in fish could be due to selective accumulation from the food rather than from bioisomerization. However, results presented in Table 4.4 show that all three diastereoisomers were below their respective MDLs at day 168 in the control fish and support the hypothesis that *in vivo* bioisomerization is responsible for the diastereoisomer specific accumulation in fish. We also determined the concentrations of the diastereoisomers in the food at two different time points (day 168 and three months after completion of the experiment) and compared it to the concentrations in food at the start of the experiment. No statistically significant

differences in the concentrations were observed in any of the foods suggesting that only the diastereoisomer added to the food was present in any significant amounts and that no *in situ* transformations occurred throughout the duration of the experiment.

Table 4.7. Bioisomerization Results[a] (arithmetic means ± standard error) on days 56 and 168 (*n=4*) [b]

Isomer fed to fish	α–HBCD nmol (p-value)[c]		β–HBCD nmol (p-value)		γ–HBCD nmol (p-value)	
	Day 56	Day 168	Day 56	Day 168	Day 56	Day 168
α	0.97 ± 0.2	0.27 ± 0.05	0.10 ± 0.05 (0.2)	<MDL[d]	0.20 ± 0.07 (0.3)	0.03 ± 0.009 (<0.06)
β	0.08 ± 0.03 (0.9)	0.16 ± 0.03 (<0.002)	0.33 ± 0.06	0.8 ± 0.03	0.07 ± 0.06 (0.9)	0.07 ± 0.01 (0.01)
γ	0.03 ± 0.01 (0.2)	0.11 ± 0.02 (<0.004)	0.009 ± 0.0009 (0.3)	<MDL[d]	0.30 ± 0.07	0.09 ± 0.005
Control	0.08 ± 0.04	<MDL[d]	0.02 ± 0.02	<MDL[d]	0.08 ± 0.07	<MDL[d]

[a]values are control corrected; [b] outliers were removed using the Q-test method (*39*) prior to statistical treatment of the data; [c]result of two-tailed t-test performed on nmoles of diastereoisomer formed by bioisomerization and amount of nmoles of the diastereoisomer in the control fish; [d]for statistical purposes, a concentration of ½ of the MDLs was assumed in those instances where diastereoisomers were below MDLs

Figure 4.7 is a sample chromatogram of a control fish extract at day 112 and Figure 4.8 is a chromatogram of a fish exposed exclusively to the β–isomer. The latter ion chromatogram clearly shows the presence of the two bioformed isomers.

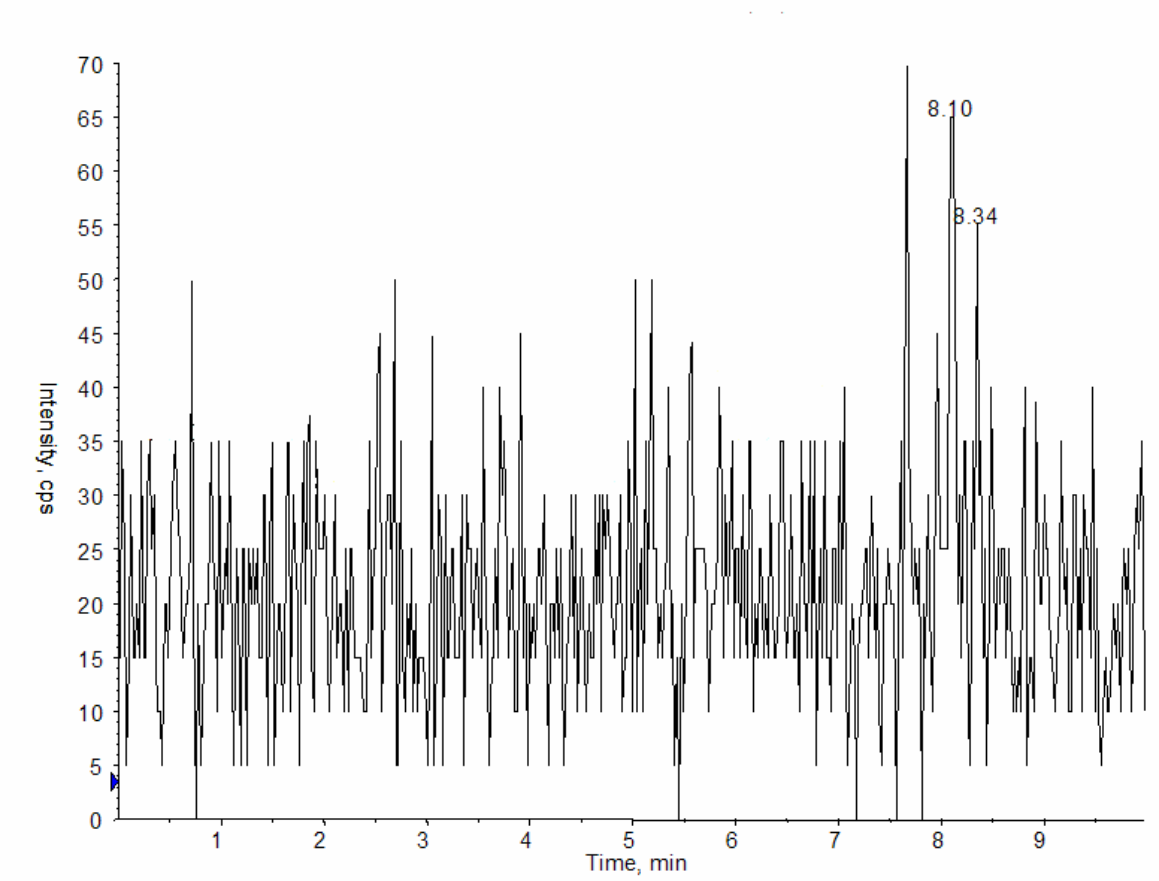

Figure 4.7. Chromatogram of extract from muscle tissue of juvenile rainbow trout, fed exclusively the unfortified (control) food, at day 112 of the depuration phase

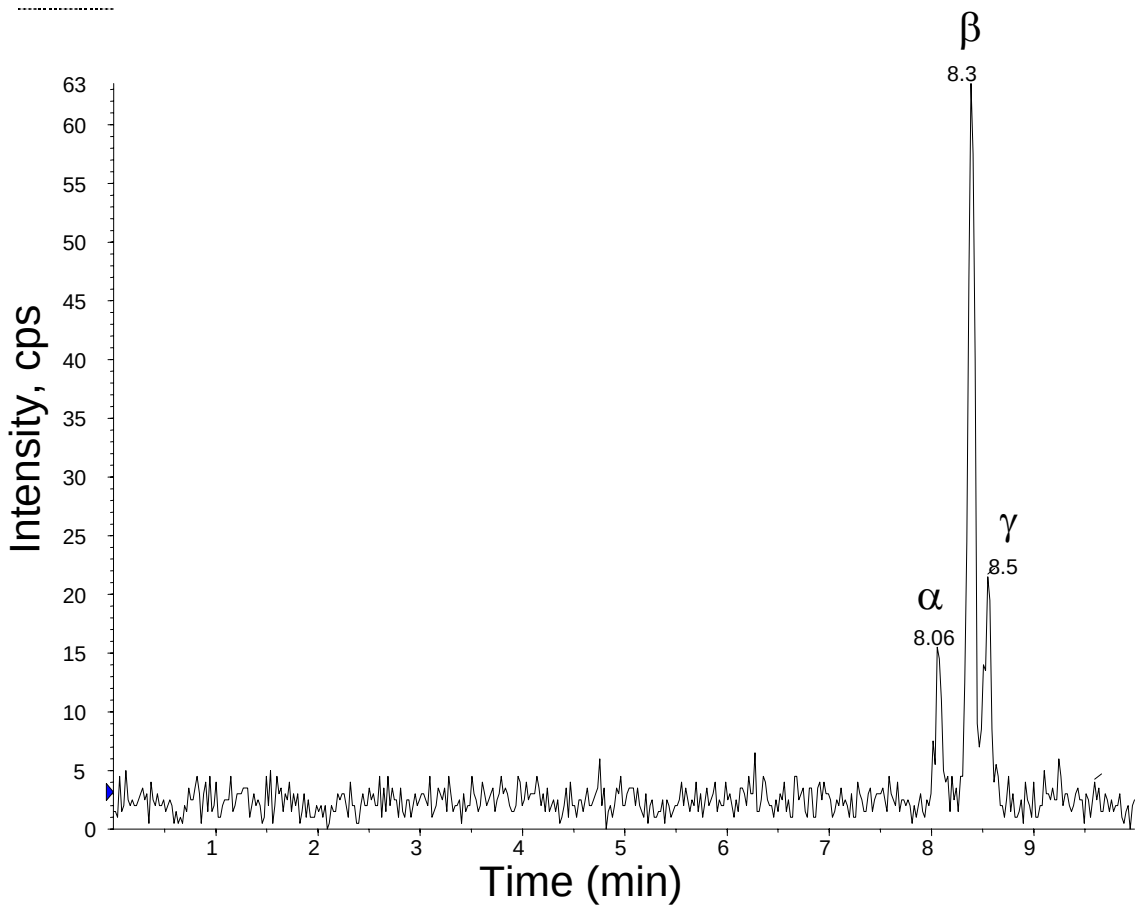

Figure 4.8. Chromatogram of extract from muscle tissue of juvenile rainbow trout, fed exclusively β-HBCD, at day 112 of the depuration phase

4.8. METABOLITES

Debromination of BDEs has been reported in the literature (*31,40*)**.** Zegers *et al*. have also reported that hydroxylated metabolites of HBCD can be isolated from fish tissues (*22*). Presence of cyctochrome P450 mediated metabolites in liver and muscle tissue was achieved using the same LC conditions and by monitoring the $[M\text{-}H+O]^-$ (*m/z* 656.6) $\rightarrow$ Br^- (*m/z* 79) MRM ion transition as described by Zegers *et al. (22)*. Muscle samples (*n=2*) were taken from both control and exposed fish on days 56, 63, 70, 112 and 168

while liver samples (*n=2*) were selected on days 56 and 168. Debromination metabolites were also investigated in the liver and muscle tissues by monitoring for possible losses of 1 Br-atom ($[M\text{-}H\text{-}Br]^-$ (*m/z* 560.7) $\rightarrow$ Br^- (*m/z* 79 and 81)) and 2-Br atoms ($[M\text{-}H\text{-}Br_2]^-$ (*m/z* 482.82) $\rightarrow$ Br^- (*m/z* 79 and 81)) from the hexabrominated parent molecule.

No peaks from debrominated or OH-HBCD metabolites were found in the monitored ions of either the muscle or liver tissue extracts. If both debromination or OH-HBCD metabolites are present at small concentrations and there is ion signal suppression because of the matrix then the ion signal from these metabolites may get masked and result in non detects.

SUMMARY

All three isomers accumulated and depurated at different rates throughout the duration of the experiment. The α–isomer was found to have the largest BMF (BMF = 4.1), followed by the γ–isomer ($t_{1/2}$ = 84 ± 51 days; BMF= 3.6) and the β–isomer ($t_{1/2}$ = 94 ± 25 days; BMF= 2.6). Because the depuration of the α–isomer did not follow a first order depuration kinetics we could not calculate $t_{½}$.

The β–isomer was found to bioisomerize to both the α– and γ–isomer. This observation coupled with the fact that the β–isomer is present at small amounts in the technical mixture could partially explain why this isomer is at undetectable concentrations in environmental samples. The γ–isomer was also found to bioisomerize to the α-isomer while the α–HBCD was found to be recalcitrant to bioisomerization. Selective biotransformation of HBCD isomers can partly explain differences observed in the isomer distribution in environmental samples but our results strongly support our hypothesis of *in vivo* bioisomerization in a teleost fish species. At this stage, it remains unclear what enzyme system(s) is/are responsible for these observations. Nevertheless, selective bioisomerization undoubtedly plays a critical role in the diastereoisomer distribution of HBCD in environmental biota.

The sampling method of this experiment could be improved; tagging the fish at the start of the experiment would improve the growth rate data, more sampling points during the

the uptake phase (a day 28) and a longer exposure time to determined when steady-state was reached.

Future work on HBCD would be to examine which enzyme system(s) are involved in the bioisomerization process. Also, the toxicity of HBCD needs to be evaluated further as HBCD is bioaccumulating in the environment and has been reported in human breast milk.

LITERATURE CITED

1. Birnbaum, L. S.; Staskal, D. F. Brominated Flame Retardants: Cause for Concern? *Environmental Health Perspectives*, **2004,** *112 (1)*, 9-17.

2. Alaee, M.; Arias, P.; Sjödin, A.; Bergman, A. An overview of commercially used brominated flame retardants, their applications, their use patterns in different countries/regions and possible modes of release. *Environment International*, **2003,** *29*, 683-689.

3. Heeb, N. V.; Schweizer, W. B.; Kohler, M.; Gerecke, A. C. *1,2,5,6,9,10-Hexabromocyclododecane - a class of compounds with a complex stereochemistry*; Presented at the Third International Workshop on Brominated Flame Retardants; Toronto, Ontario, Canada, June 2004; 337-339.

4. de Wit, C. An overview of brominated flame retardants in the environment. *Chemosphere*, **2002,** *46*, 583-624.

5. Peled, M., Scharia, R., and Sondack, D. Thermal rearrangement of hexabromocclododecane (HBCD); *Advances in Organobromine Chemistry II;* Elsevier Publishing Company Inc.: Amsterdam, 1995; 92-99.

6. Tomy, G. T.; Budakowski, W.; Halldorson, T.; Whittle, M. D.; Keir, M. J.; Marvin, C.; MacInnis, G.; Alaee, M. Biomagnification of α- and γ-Hexabromocyclododecane isomers in a Lake Ontario Food Web. *Environmental Science and Technology*, **2004,** *38 (8)*, 2298-2303.

7. Arsenault, G.; Chittim, B.; McAlees, A.; McCrindle, R. *A three dimensional view of the alpha- and gamma- 1,2,5,6,9,10-Hexabromocyclododecane conformers with the help of nuclear magnetic resonance spectral characterization and semi-empirical calculations*; Presented at the Third International Workshop on Brominated Flame Retardants; Toronto, Ontario, Canada, June 2004; 305-308.

8. American Chemistry Council. *Data Summary and test plan for hexabromocyclododecane (HBCD) Case No. 3194556*; Report No. AR201-13459A; 2001; Brominated Flame Retardant Industry Panel (BFRIP), Arlington, VA..

9. The National Academies Press. Toxicological risks of selected flame retardant chemicals, 2000; http://www.nap.edu/openbook/0309070473/html/53.html .

10. Remberger, M.; Sternbeck, J.; Palm, A.; Kaj, L.; Strömberg, K.; Brorström-Lundén, E. The environmental occurrence of hexabromocyclododecane in Sweden. *Chemosphere*, **2004,** *54*, 9-21.

11. Stenzel, J. J.; Markley, B. J. *Hexabromocyclododecane (HBCD); Determination of the water solubility*; Report No. 439C-105; 1997; Brominated Flame Retardant Industry Panel (BFRIP), Arlington, VA.

12. Hunziker, R. W.; Gonsior, S.; MacGregor, J. A.; Desjardins, D.; Ariano, J.; Friederich, U. *Fate and Effect of Hexabromocyclododecane in the Environment*; Organohalogen Compounds, **2004**; *66,* 2300-2305.

13. Lassen, C.; Løkke, S.; Andersen, L. I. *Brominated flame retardants substance flow analysis and assessment of alternatives*;1999; Danish Environmental Protection Agency, Denmark.

14. Zitko, V. Expanded Polystyrene as a Source of Contaminants. *Marine Pollution Bulletin*, **1993,** *26*, 584-585.

15. Reyes, J. D.; Scheinert, J.; Georlette, P. HBCD: Advancing Performance through innovation. *Recent advances in flame retardancy of polymer materials*, **1997,** *8*, 390-399.

16. Bromine Science and Environmental forum. Hexabromocyclododecane (HBCD) fact Sheet, 2003 ed., http://www.bsef-site.com/docs/BSEf%20factsheet%20HBCD%20A4%2030%20sept%202003.pdf in www.bsef.com .

17. Kesner, M.; de Vos, W. Teaching about flame retardants. A joint Israeli-Dutch project. *Journal of Chemical Education*, **2001,** *78 (1)*, 41-45.

18. Bergman, Å. *BFRs- with focus on Environmental Fate and Risks of Decabromodiphenyl ether and Hexabromocyclododecane*; Presented at the Third International Workshop on Brominated Flame Retardants; Toronto, Ontario, Canada, June 2004; 1-5.

19. Law, R.; Allchin, C.; de Boer, J.; Covaci, A.; Herzke, D.; Lepom, P.; Morris, S.; de Wit, C. *Levels and Trends of Brominated Flame Retardants in the European*

Environment; Presented at the Third International Workshop on Brominated Flame Retardants; Toronto, Ontario, Canada, June 2004; 79-104.

20. Morris, S.; Allchin, C.; Zegers, B.; Haftka, J. J .H.; Boon, J.; Belpaire, C.; Leonards, P. E. G.; Van Leeuwen, S. P. J.; de Boer, J. Distribution and fate of HBCD and TBBPA brominated flame retardants in north sea estuaries and aquatic food webs. *Environmental Science and Technology*, **2004,** *38 (21)*, 5497-5504.

21. Sellstrom, U.; Kierkegaard, A.; de Wit, C.; Jansson, B. Polybrominated diphenyl ethers and hexabromocyclododecane in sediment and fish from a Swedish river. *Environmental Toxicology and Chemistry*, **1998,** *17 (6)*, 1065-1072.

22. Zegers, B. N.; Mets, A.; van Bommel, R.; Minkenberg, C.; Hamers, T.; Kamstra, J. H.; Pierce, G. J.; Boon, J. P. Levels of hexabromocyclododecane in harbor porpoises and common dolphins from western European seas, with evidence for stereoisomer-specific biotransformation by cytochrome P450. *Environmental Science and Technology*, **2005**, 39(7), 2095-2100.

23. Law, K.; Halldorson, T.; Danell, R.; Stern, G.; Gewurtz, S.; Alaee, M.; Marvin, C.; Whittle, M. D.; Tomy, G. Bioaccumulation and trophic transfer of some brominated flame retardants in a Lake Winnipeg food web. *Environmental Science and Technology*, **2006**, submitted for publication.

24. Ronisz, D; Finne, E. F.; Karlsson, H.; Förlin, L. Effects of the brominated flame retardants hexabromocyclododecane (HBCDD), and tetrabromobisphenol A (TBBPA), on hepatic enzymes and other biomarkers in juvenile rainbow trout and feral eelpout. *Aquatic Toxicology,* **2004**, 69, 229-245.

25. Helleday, T.; Tuominen, K.-L.; Bergman, Å.; Jenssen, D. Brominated flame retardants induce intragenic recombination in mammalian cells. *Mutation Research*, **1999,** *439*, 137-147.

26. Darnerud, P. O. Toxic effects of brominated flame retardants in man and in wildlife. *Environment International*, **2003,** *29*, 841-853.

27. Lind, Y.; Aune, M.; Atuma, S.; Becker, W.; Bjerselius, R.; Glynn, A.; Darnerud, P. O. Food intake of the brominated flame retardants PBDEs and HBCD in Sweden. *Organohalogen Compounds*, **2002,** *58*, 181-184.

28. Budakowski, W. R.; Tomy, G. T. Congener-specific analysis of hexabromocyclododecane by high-performance liquid

chromatography/electrospray tandem mass spectrometry. *Rapid Communications in Mass Spectrometry*, **2003,** *17*, 1399-1404.

29. Tomy, G.; Halldorson, T.; Danell, R.; Law, K.; Arsenault, G.; Alaee, M.; MacInnis, G.; Marvin, C. Refinements to the isomer specific method for the analysis of hexabromocyclododecane (HBCD), *Rapid Communications in Mass Spectrometry*, **2005**, 19, 2819-2826.

30. Barontini, F.; Cozzani, V.; Petarca, L. Thermal stability and decomposition products of hexabromocyclododecane. *Industrial and Engineering Chemistry Research*, **2001,** *40*, 3270-3280.

31. Tomy, G. T.; Palace, V. P.; Halldorson, T.; Braekevelt, E.; Danell, R.; Wautier, K.; Evans, B.; Brinkworth, L.; Fisk, A. T. Bioaccumulation, Biotransformation, and Biochemical Effects of Brominated Diphenyl Ethers in Juvenile Lake Trout (*Salvelinus namaycush*). *Environmental Science and Technology*, **2004,** *38 (5)*, 1496-1504.

32. Lough, W. J.; Wainer, I. W. *Liquid performance liquid chromatography fundamental principles and practice*, Blackie Academic & Professional: London. 1996.

33. Willoughby, R.; Sheehan, E.; Mitrovich, S. *A global view of LC/MS; how to solve your most challenging analytical problems*, 2nd ed.; Global View Publishing: Pittsburgh, PA. 2002.

34. Parris, N. A. *Instrumental liquid chromatography; a practical manual on high-performance liquid chromatographic methods*, 2nd ed.; Elsevier Science Publishing Company Inc.: New York, NY. 1984.

35. Ardrey, B. *Liquid chromatography- mass spectrometry: an introduction*, John Wiley & Sons Ltd.: Sussex. 2003

36. Pramanik, B. N.; Ganfuly, A. K.; Gross, M. L. *Applied electrospray mass spectrometry*, Marcel Dekker, Inc.: New York. 2002.

37. Miller, P. E.; Denton, M. B. The quadrupole mass filter: Basic operating concepts. *Journal of Chemical Education*, **1986,** *63 (7)*, 617-622.

38. Palace, V.; Law, K.; Halldorson, T.; Danell, R.; Wautier, K.; Evans, B.; Brinkworth, L.; Alaee, M.; Marvin, C.; Tomy, G. Dietary accumulation of hexabromocyclododecane diastereoisomers in juvenile rainbow trout

(Oncorhynchus mykiss) II: biochemical effects. *Environmental Toxicology and Chemistry*, **2006,** To be submitted.

39. Dean, R. B.; Dixon, W. J. Simplified Statistics for Small Numbers of Observations. *Analytical Chemistry*, **1951,** *23 (4)*, 636-638.

40. Stapleton, H. M.; Alaee, M.; Letcher, R. J.; Baker, J. E. Debromination of the Flame Retardant Decabromodiphenyl Ether by Juvenile Carp (*Cyprinus carpio*) following Dietary Exposure. *Environmental Science and Technology*, **2004,** *38 (1)*, 112-119.

APPENDIX A

1. Sample Calculations;

These calculations were used to calculate the lipid corrected native isomer concentrations in the fish muscle and the food. These calculations were done individual for each isomer.

Areas are the electronically integrated peak areas from the ion chromatograms determined by Analyst Software

A.1.1Percent Recovery;

$$\%\ rec = \left(\frac{CA\ {}^{13}C_{12}\ SA}{area\ of\ {}^{13}C_{12}\ STD} \right) \times 100$$

$$CA\ {}^{13}C_{12}\ SA = area\ {}^{13}C_{12}\ SA \times \left(\frac{8mL}{7mL} \right) \times \left(\frac{area\ d_{18}\ STD}{area\ d_{18}\ SA} \right)$$

[a] a 1mL portion of a 8mL sample was used for gravimetrical lipid determination (see Figure 3.1)

A.1.2Amount of Native HBCD in sample in pg;

$$Native\ HBCD\ (pg\ total) = \left(\frac{CA\ Native\ SA \times 75\,pg}{Area\ Native\ STD} \right) \times \left(\frac{200\,\mu L}{3\,\mu L} \right)$$

[b]75 pg is the amount of native HBCD in the external standard
[c] 200 µL is the final volume of the sample; 3 µL is the volume of sample injected onto the HPLC column

$$CA\ native\ HBCD\ SA = Native\ area \times \left(\frac{area\ d_{18}\ STD}{area\ d_{18}\ SA} \right) \times \left(\frac{100}{\%\ rec} \right) \times \left(\frac{8mL}{7mL} \right)$$

A.1.3Amount of Native HBCD in sample in ng;

$$Native\ HBCD\ (ng\ total) = \frac{Native\ HBCD\ (pg\ total)}{1000}$$

A.1.4Concentration (ng/g) of Native HBCD on a wet weight basis;

$$Native\ HBCD\ (ng/g, wet\ weight) = \frac{Native\ HBCD\ (ng\ total)}{wet\ weight\ of\ sample}$$

A.1.5Percent lipid;

$$\%\ lipid = \frac{lipid(g) \times 8mL}{wet\ weight\ of\ sample} \times 100$$

A.1.6Lipid corrected concentration (ng/g) of Native HBCD;

$$Native\ HBCD\ (ng/g, lipid\ corrected) = \frac{Native\ HBCD\ (ng/g, wet\ weight)}{\%lipid} \times 100$$

A.1.7Amount (nmoles) of Native HBCD in the muscle tissue that was extracted;

$$nmoles = \frac{concentration(ng/g) \times weight\ of\ fish\ muscle\ extracted}{molecular\ weight\ of\ HBCD(g/mole)}$$

[a] molecular weight of HBCD = 641 g/mole

APPENDIX B

1. Example calculations for an exclusively β–isomer fed fish at day 112 of the depuration phase of the experiment;

β-isomer	Area read off of chromatogram
$^{13}C_{12}$ in the SA	$2.88e^{+4}$
$^{13}C_{12}$ in the external STD	$3.18e^{+4}$
d_{18} in the SA	$2.92e^{+4}$
d_{18} in the STD	$2.40e^{+4}$
Native β-isomer in the SA	$2.69e^{+3}$
Native β-isomer in the STD	$1.07e^{+4}$

Weight of muscle tissue extracted= 15.03g

Weight of lipid in 1 mL= 0.0251g

B.1.1Percent Recovery;

$$CA\ ^{13}C_{12}\ SA = 2.88e^{+4} \times \left(\frac{8mL}{7mL}\right) \times \left(\frac{2.40e^{+4}}{2.92e^{+4}}\right)$$

CA $^{13}C_{12}$ SA= $2.99e^{+4}$

$$\%\ rec = \left(\frac{2.71e^{+4}}{3.18e^{+4}}\right) \times 100$$

% rec = 85.2%

B.1.2Amount of Native HBCD in sample in pg;

$$CA\ native\ HBCD\ SA = 2.69e^{+3} \times \left(\frac{2.40e^{+4}}{2.92e^{+4}}\right) \times \left(\frac{100}{85.2}\right) \times \left(\frac{8mL}{7mL}\right)$$

CA native HBCD SA= $2.97e^{+3}$

$$Native\ HBCD\ (pg\ total) = \left(\frac{2.97e^{+3} \times 75pg}{1.07e^{+4}}\right) \times \left(\frac{200\mu L}{3\mu L}\right)$$

Native HBCE (pg total) = $1.39e^{+3}$ pg

B.1.3Amount of Native HBCD in sample in ng;

$$Native\ HBCD\ (ng\ total) = \frac{1.39e^{+3}\,pg}{1000}$$

Native HBCD (ng total) = 1.39 ng

B.1.4Concentration (ng/g) of Native HBCD on a wet weight basis;

$$Native\ HBCD\ (ng/g, wet\ weight) = \frac{1.39ng}{15.03g}$$

Native HBCD (ng/g, wet weight) = $9.25e^{-2}$ ng/g

B.1.5Percent lipid;

$$\%\ lipid = \frac{0.0251g \times 8mL}{15.03g} \times 100$$

% lipid = 1.34%

B.1.6Lipid corrected concentration (ng/g) of Native HBCD;

$$Native\ HBCD\ (ng/g, lipid\ corrected) = \frac{9.25e^{-2} ng/g}{1.34\%} \times 100$$

Native HBCD (ng/g, lipid corrected)= 6.90 ng/g (lipid corrected)

B.1.7 Amount (nmoles) of Native HBCD in the muscle tissue that was extracted;

$$nmoles = \frac{6.90 ng/g \times 15.03 g}{641 (g/mole)}$$

nmole= $1.62e^{-1}$ nmoles